PROGRESSING TOWARDS A PHOTOSWITCHABLE KARSTEDT'S CATALYST

by

Soizic Wadge
Bachelor of Science, University of Victoria 2006

THESIS SUBMITTED IN PARTIAL FULFILLMENT OF
THE REQUIREMENTS FOR THE DEGREE OF

MASTER OF SCIENCE

In the
Department of Chemistry

SIMON FRASER UNIVERSITY

Summer 2009

APPROVAL

Name: **Soizic Guevel Ruth Wadge**

Degree: **Master of Science**

Title of Thesis: **Progressing towards a photoswitchable Karstedt catalyst**

Examining Committee:

Chair:

_____

Senior Supervisor
Dr. Neil Branda
Professor

_____

Committee Member
Dr. Robert Britton
Assistant Professor

_____

Committee Member
Dr. Gary Leach
Associate Professor

_____

Internal Examiner
Dr. Steve Holdcroft
Professor

_____

Date Defended/Approved: May-21-2009

Declaration of
Partial Copyright Licence

ABSTRACT

Release coatings, an important industrial product, are made of polysiloxanes, which are synthesized by hydrosilylation reactions that are commonly catalyzed by Karstedt's catalyst. For manufacturing purposes, control over Karstedt's catalyst is required. This is achieved by inhibiting the active catalyst, which can then be triggered by heating. A more energy efficient method could be achieved by activating the catalyst with light instead of heat. Dithienylethene molecular switches are well-suited to the development of photo-reactive systems since they have well-behaved photochromic properties. Dithienylethene derivatives exhibit significant differences between their ring-open and ring-closed isomers. Control over the initiation of Karstedt's catalyst with light may be achieved, by modifying a dithienylethene such that one isomer acts as an inhibitor while the other does not. This thesis presents novel approaches to the inhibition of Karstedt's catalyst. Furthermore, the characteristics necessary for a photoswitchable inhibitor are well defined and a method for identifying potential inhibitors is presented.

Keywords: Karstedt's catalyst, release coatings, controlling reactivity, photochemistry, hydrosilylation.

DEDICATION

To mom and dad, the best parents I could have asked for.

ACKNOWLEDGEMENTS

I would like to thank my senior supervisor Neil Branda for his guidance and motivation. In addition, I extend my thanks to the members of my supervisory committee, Gary Leach, Robert Britton, as well as my internal examiner Steve Holdcroft for their helpful advice and for allowing me to improve not only as a scientist, but also as a writer. A special thanks to all the members of the Branda group both past and present for their advice and support.

I would also like to thank Andrew Lewis and Colin Zang for NMR services as well as Susie Smith for all sorts of help during my degree.

Finally, a big thank you to my mom and dad. To my mom for giving me opportunities she never had, and to my dad for sharing his love of science. And to Peter, thanks for putting up with me, I love you.

TABLE OF CONTENTS

LIST OF FIGURES

LIST OF TABLES

LIST OF SCHEMES

LIST OF EQUATIONS

LIST OF ABBREVIATIONS

δ	chemical shift
Δ	heating
λ	wavelength
λ_{max}	wavelength at the absorption maximum in a given region
μL	microlitre
°C	degree Celsius
AcOH	acetic acid
bd	broad doublet
bm	broad multiplet
bs	broad singlet
C	carbon
C	complex (when reffering to gues-host complexes)
cm	centimetre
d	doublet
dd	doublet of doublets
dm	doublet of multiplets
DMF	*N*,*N*-dimethylformamide
DMSO	dimethylsulfoxide
dt	doublet of triplets
DCE	dichloroethane
DCTE	dicyanoethylene-thienylethene
DTE	dithienylethene
DVTMS	divinyltetramethyldisiloxane
eq.	equivalents
Et_2O	diethyl ether
EtOAc	ethyl acetate
exp.	experimental
g	gram
GC	gas chromatography

G	guest
h	hour
H	host
H	proton
HOMO	highest occupied molecular orbital
hν	photon energy
Hz	Hertz
J	coupling constant
k	forward reaction rate constant
k’	backward reaction rate constant
K	equilibrium constant
LUMO	lowest unoccupied molecular orbital
m	multiplet
M	mole/litre
m.p.	melting point
Me	methyl
mg	milligram
MHz	megahertz
min	minute
mL	millilitre
mmol	millimole
MS	mass spectrometry
mol	mole
n-Buli	*n*-butyllithium
NBS	*N*-bromosuccinimide
nm	nanometre
NMR	nuclear magnetic resonance
Ph	phenyl
ppm	part per million
PSS	photostationary state
s	singlet (when used in NMR spectroscopy)

s	second
T	temperature
t	triplet
t-BuLi	*tert*-butyllithium
THF	tetrahydrofuran
TLC	thin layer chromatography
UV	ultraviolet
UV-vis	ultraviolet-visible
vis	visible

1 INTRODUCTION

1.1 Release Coatings

1.1.1 What Are Release Coatings ?

Release coatings are polymer coatings used as non-stick backings for stamps, labels and envelopes and allow for their removal effortlessly while retaining their adhesive properties. As shown in *Figure 1.1,* a release coating is applied to a substrate (usually paper), as a result, adhesives can be peeled easily from the coated surface. Depending on the application, release coatings can be manufactured according to customer specifications; these include coating thickness, release force and rigidity. Each year, twenty-two million square kilometres of release coatings are produced worldwide, which is enough to cover all of Canada twice.[1] Release coatings comprise a billion dollar industry and most major chemical manufactures have release coating divisions including, but not limited to, Dow Corning, General Electric, and DuPont.

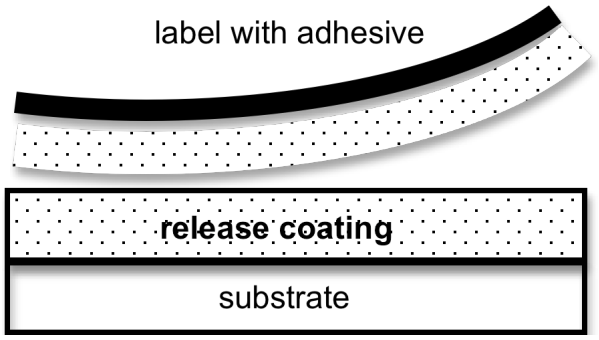

Figure 1.1 Release coatings allow for easy removal of adhesives from the coated surface with no adhesion between the coating and an adhesive layer.

1.1.2 Release coatings are made of polysiloxanes

Release coatings are most commonly made of polysiloxanes (*Figure 1.2*), which are polymers containing Si-O bonds along the backbone of the polymer chain. Polysiloxanes are used for their low release force; which is the force required to remove an adhesive from its backing. The low release force is due to low surface tension, and polysiloxanes have the lowest surface tension of all known polymers with the exception of Teflon.[2,3] The low surface tension is a direct result of the high flexibility of the siloxane chain, which adopts a low surface energy conformation, whereby the hydrophobic pendant groups (**R** in *Figure 1.2*) bonded to the silicon surround the backbone of the polymer in a cylindrical manner. The chain flexibility is attributed to the low energy rotation barrier of the Si-O bond.[4,5]

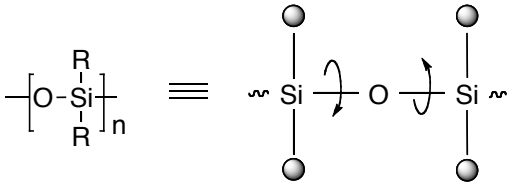

Figure 1.2 Typical siloxane polymer which contains Si-O bonds along the backbone. In polydimethylsiloxane R = methyl.

1.1.3 Hydrosilylations

Polysiloxanes are made by hydrosilylation reactions, through the addition of a silane group across an unsaturated carbon-carbon bond. A common release coating is made by crosslinking a short chain silane-functionalized polydimethylsiloxane (PDMS) polymer (**1.1**) with another short chain vinyl-functionalized PDMS polymer (**1.2**). The amount of vinyl or silane functionalization on the PDMS polymer depends on the degree of crosslinking desired, but is generally around 0.5 to 10 mole percent.[6] *Scheme 1.1*

shows the general equation for hydrosilylation (top), and typical materials that are used in release coatings (bottom). This reaction is often referred to as crosslinking or curing. Herein this reaction will be referred to as curing.

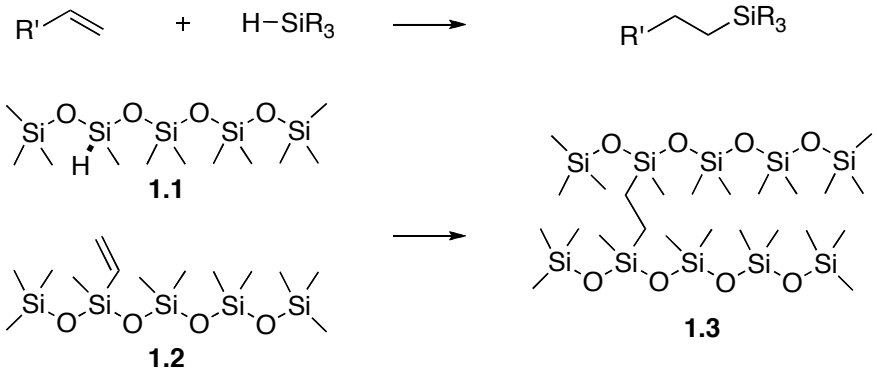

Scheme 1.1 A general hydrosilylation reaction (top), and typical PDMS functionalized reagents that are used for the reaction (bottom).

Hydrosilylation reactions are promoted by soluble platinum catalysts such as platinum on carbon, Speier's catalyst (H_2PtCl_6), and Karstedt's catalyst (*Scheme 1.2*). Karstedt's catalyst is the most active of the three and is currently the most widely used in industry.[7] This catalyst consists of a platinum centre coordinated to siloxane ligands and is most commonly depicted as a dimer (*e.g* **1.4**); however, it has been demonstrated that other platinum complexes (*e.g* **1.6** and **1.7**) do exist in equilibrium with the dimer **1.4**.[8,9] Dimer **1.4** is often referred to as the "pre-catalyst", while complex **1.7** is known to be the active catalyst that enters the catalytic cycle.[9]

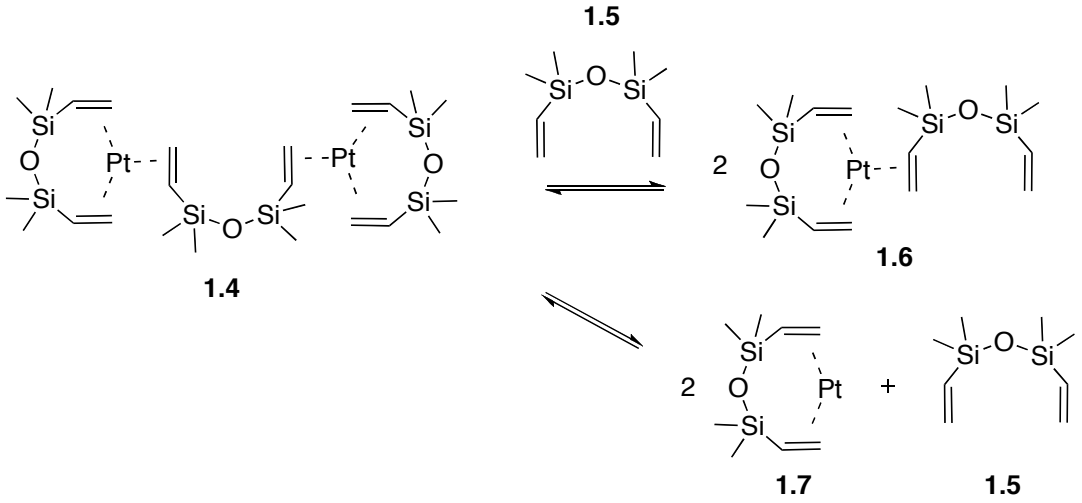

Scheme 1.2 Karstedt's catalyst is a platinum-siloxane complex, most commonly depicted as a dimer (**1.4**), but is also known to be in equilibrium with complexes **1.6** and **1.7**.

Hydrosilylation reactions can be described by the Chalk-Harrod catalytic cycle. *Scheme 1.3* shows the general catalytic cycle for the hydrosilylation of alkenes by platinum as well as other late transition metals such as palladium and nickel.[10]

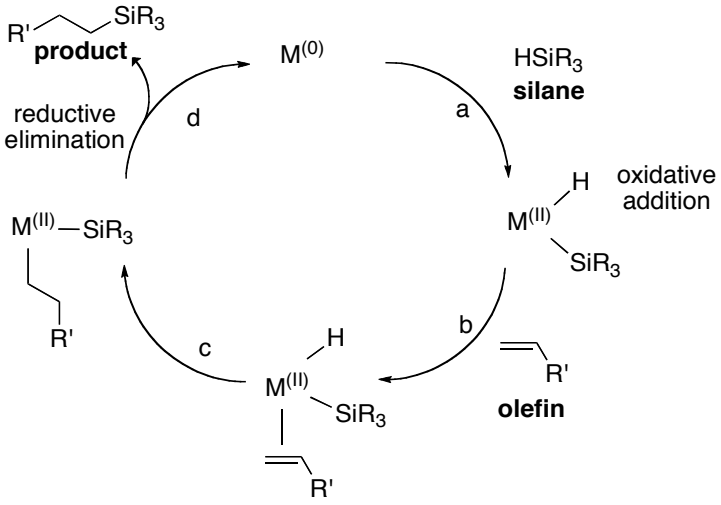

Scheme 1.3 The Chalk-Harrod catalytic cycle for the hydosilylation ok alkenes by late transitions metals.

As illustrated in *Scheme 1.3*, the Chalk-Harrod catalytic cycle begins with the oxidative addition of the silane to the metal centre (a) which generates a $M^{(II)}$ species.

Coordination of the olefin to the metal centre (b) is followed by the insertion of the olefin into the $M^{(II)}$-H bond (c), followed by reductive elimination of the product (d). While most hydrosilylation reactions follow the Chalk-Harrod mechanism, this process does not account for some observed trends such as the formation of colloidal species, that will be discussed further in *Chapter 2*.

1.1.4 Manufacturing of Release Coatings

Manufacturing of release coatings on an industrial scale is not a simple task. The main concern of process chemists is the bath life of the starting materials, which refers to the length of time that the reagents and the catalyst must remain in their liquid form without curing. Because the paper must be coated with starting materials and then cured, the starting materials must remain unreacted for a prolonged period of time without hardening.

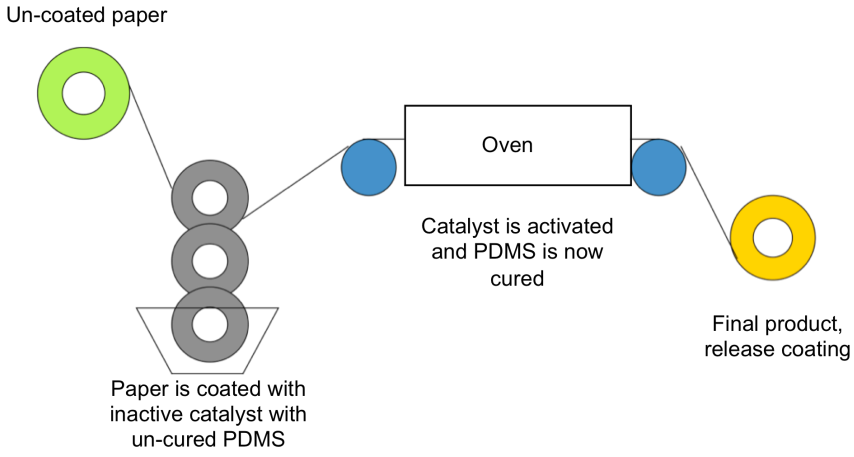

Figure 1.3 Illustration of the manufacturing process for release coatings. Paper is coated with un-cured PDMS and inhibited Karstedt catalyst. The paper is then passed through an oven, which initiates the catalyst and allows for curing.

As illustrated in *Figure 1.3,* the manufacturing process of release coatings begins with the untreated paper, which is dipped in a bath and coated with a mixture of un-cured PDMS and catalyst in its inactive state. Subsequently, the treated paper is passed through an oven, which activates the catalyst and allows for the curing of the PDMS. Finally, the paper is then cooled, rolled and is ready for use.

In the manufacturing of release coatings two methods have been used. The first being microencapsulation, in which the catalyst is encapsulated in a thermoplastic such as polyethylene or polystyrene and added to the unreacted reagents (vinyl/silane functionalized PDMS). Upon heating, the polymer dissolves and releases the catalyst into the reagent solution. Although encapsulation achieves necessary bath life requirements, the dissolution of capsules is often not homogeneous and results in uneven curing of the polymer.[11]

An alternative to microencapsulation is to add the catalyst to the reagent solution in an inactive state and then use an external stimulus to activate the catalyst. This approach (often referred to as command-cure) uses an inhibitor, which inhibits the catalyst by coordinating to the metal centre (*Figure 1.4*). Consequently, the catalyst can be added to the reactants without curing. The paper is coated with this solution (uncured PDMS), and as it is passed through an oven, the inhibitor is released, which in turn activates the catalyst and allows for curing.[12] A number of inhibitors for Karstedt's catalyst have been developed; of these, dimethyl fumarate and dimethyl maleate are the most common.[13,14] This command-cure method is the most common method for the manufacturing of release coatings.

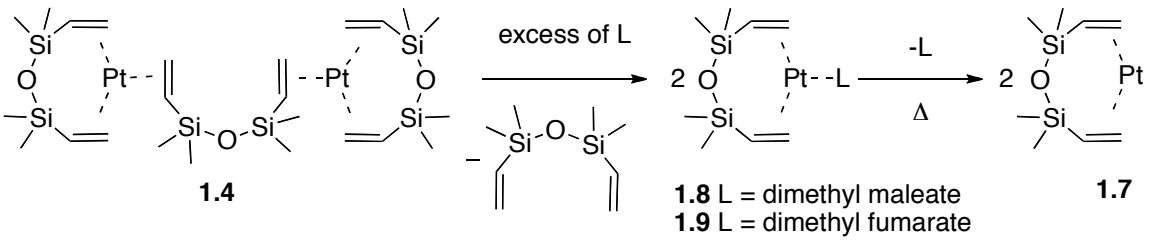

Figure 1.4 The addition of inhibitor ligands to Karstedt's catalyst, upon heating the inhibitor is released and the active catalyst is generated.

1.1.5 Inhibiting Karstedt's Catalyst

The command-cure system described above works by inhibiting Karstedt's catalyst through the addition of a fumarate or a maleate ligand. Stabilization of the catalyst is key to designing ligands that both inhibit and improve the catalyst. On the one hand, ligands that stabilize the catalyst to a small degree can actually improve the efficiency of the catalyst by extending its lifetime; on the other hand, the catalyst can become so stable that it is no longer active. In command-cure systems, the inhibitor ligand must be of intermediate strength, potent enough to inhibit the catalyst at room temperature, but not so effective that the catalyst can not be activated by heating. Any ligand that competes with the added olefin (reactant) for a site on the platinum is considered an inhibitor, whereas a ligand that excludes other olefins from coordinating to the platinum is a poison.[15]

Karstedt's catalyst is stabilized by strongly coordinating ligands, most of which possess the ability to back-bond to the metal centre (see *Section 1.1.6*).[16] As illustrated in *Figure 1.5,* when naphthylquinone is used as a ligand it coordinates to the platinum better than the DVTMS ligand, resulting in a slightly more active catalyst. At the other extreme, the tetracyanoethylene ligand, coordinates so strongly to the platinum centre that it

"poisons" the catalyst and is of no practical use for a command-cure application. Dimethyl fumarate, shown in the middle, acts as the "happy medium" for the purpose of command-cure applications, as it is an inhibitor at room temperature, however upon heating, the active catalyst is released.

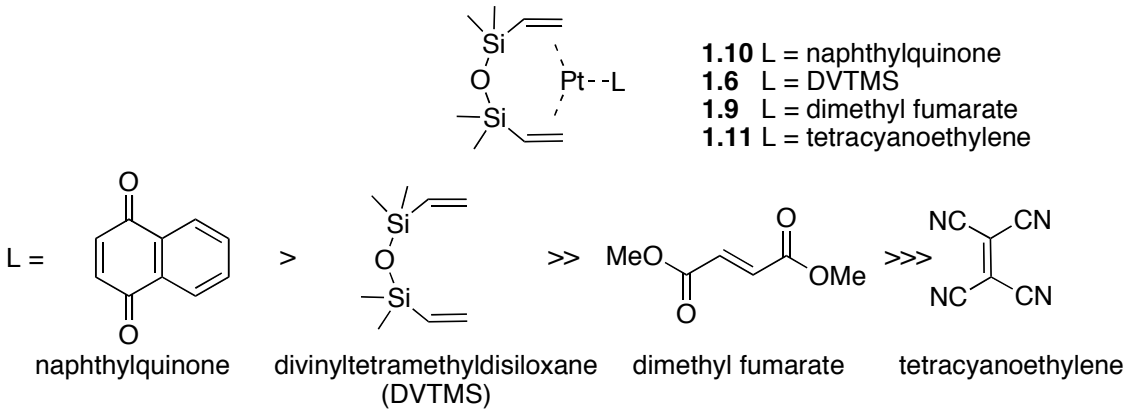

Figure 1.5 Examples of Karstedt type catalysts shown in order of reactivity.

The command-cure system is inherently flawed, since only inhibitors of moderate strength can be used. The requirement for a long bath life must be balanced with the need for moderate initiation temperatures (60-100 °C). Inhibitors that provide long bath lives often require high curing temperatures while inhibitors with lower initiation temperatures result in shorter bath lives.

1.1.6 Mode of Inhibition

In the previous section it was stated that ligands that coordinate strongly to a metal centre result in better inhibition of Karstedt's catalyst. This section will explore how that coordination takes place. A common feature of maleate and fumarate ligands (as well many other Karstedt catalyst inhibitors) is the presence of an electron deficient alkene. Lewis *et. al.* has shown that the electron deficient olefin bonds directly to the

platinum centre in a η^2 fashion and that all the ligands are arranged in a co-planar fashion, such that the antibonding π^* orbitals of the ligand are in the same plane as the complex (*Figure 1.6*).[17]

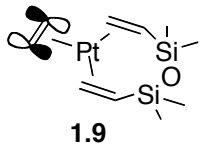

1.9

Figure 1.6 Ligand arrangement around the platinum centre in Karstedt's catalyst, fumarate has been simplified to an alkene for clarity.

In zerovalent platinum-olefin complexes, backbonding is the most important contributor to the Pt-C bond.[18] Backbonding occurs when electron density from one atom is donated into the antibonding π^* orbital of another ligand, which results in a decrease in the bond order of the ligand and an increase in the metal-ligand bond order. *Figure 1.7* shows the HOMO of the metal centre and the empty LUMO of the ligand.

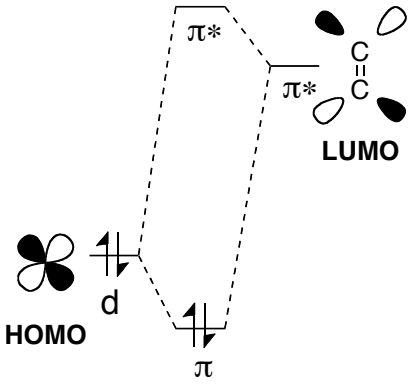

Figure 1.7 Molecular orbital diagram of backbonding which involves the donation of electron density from a metal into the empty π^* orbital of an olefin.

The ability of the olefin to accept electron density is often referred to as π-Lewis acidity. With respect to the inhibition of Karstedt's catalyst, the better the π-Lewis acidity of the ligand the better the inhibitor.[19]

1.1.7 Problems with Current Technology

Presently many problems exist with thermal curing (*i.e.* volatile inhibitors). High temperatures can curl and degrade coatings, consequently, ovens must operate at relatively low temperatures (60 °C). For sufficient curing, ovens must therefore be long (50-100 m), which represents an enormous energy cost. Furthermore, these large ovens require long warm up periods, and the product must also be cooled before it can be processed and shipped. Thermal curing also degrades many substrates, which therefore limits the range of release coatings that can be made, and lastly, thermal curing generates large amounts of volatile organic compounds (VOC's), which present environmental and safety concerns.

Currently, UV-light and electron beam (EB) curing are being used as alternatives to thermal curing. These methods rely on radical initiation and provide many advantages over thermal curing, such as greater efficiency and safety. Radiation-cured systems work by generating radicals and require functional groups such as epoxides or acrylates to be appended to the siloxane background (*Figure 1.8*). Changing the polarity of the functional groups directly affects the surface tension of the coating and as a result the release properties of the product are limited by these functional groups. Due to these reasons, radiation-cured systems only account for 15% of the release coating market (the rest are thermally-cured systems). [20]

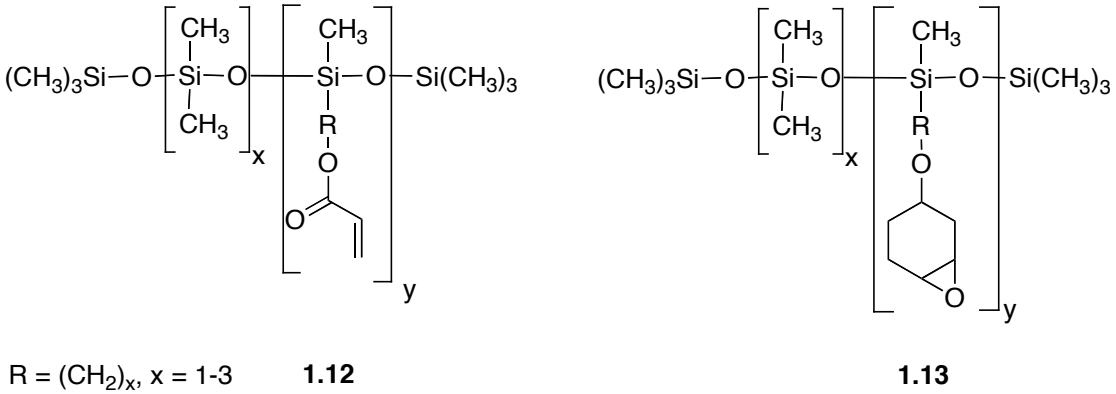

R = $(CH_2)_x$, x = 1-3 **1.12** **1.13**

Figure 1.8 Example of radiation-cured PDMS polymers containing epoxide or acrylate functional groups.

It is clear that radiation-cured systems address many of the problems of thermally-cured systems; on the other hand, thermally-cured systems are more versatile but lead to the problems as summarized in *Table 1.1*. A model system would incorporate the advantages of both methods.

Table 1.1 Summary of advantages and disadvantaged of current release coating technologies.

System	Advantages	Disadvantages
heat-cured	wide range of products	energy intensive time consuming thermal degradation of product, environmental and safety concerns.
radiation-cured	energy efficient shorter production time compact equipment less safety concerns	small number of products available

The key advantage of heat-cured systems is that they do not require specific functional groups on the PDMS chain, however, they are energy inefficient. Radiation-

cured systems are much more energy efficient but are limited in scope. This thesis proposes a combination of these two approaches by the use of a radiation initiated catalyst. By using an inhibitor that is deactivated by light, a radiation-initiated system that acts directly on the catalyst is proposed. This type of system would incorporate all the advantages of radiation-cured systems without sacrificing the versatility of heat-cured systems.

1.2 Controlling Catalysis with Light

Chemists are continually seeking new methods to obtain greater control over chemical reactions and processes. Greater control results in more efficiency and improved safety, both of which are of great interest. Heat is perhaps the most widely used reaction initiation method, however, there are many disadvantages to using heat as a method to control reactions: first, heat is non-specific and cannot distinguish between molecules. Second, heat is inefficient at delivering energy, as it is very hard to deliver in a homogeneous manner. Finally, heat is uneconomical and also poses significant safety risks in industrial settings. For these reasons, light is a very attractive alternative.

1.2.1 Photochromism

Figure 1.9 illustrates the absorption spectra for a typical photochromic molecule transforming between two forms, *A* and *B*, by the absorption of electromagnetic radiation.[21] These two forms must also have two distinct absorption spectra and the transformation can occur in one or both directions.[22] The thermodynamically stable form *A* can be converted into *B* by the absorption of the appropriate wavelength. The reverse reaction can occur thermally, in the case of T-type photochromism, or photochemically, in the case of P-type photochromism.

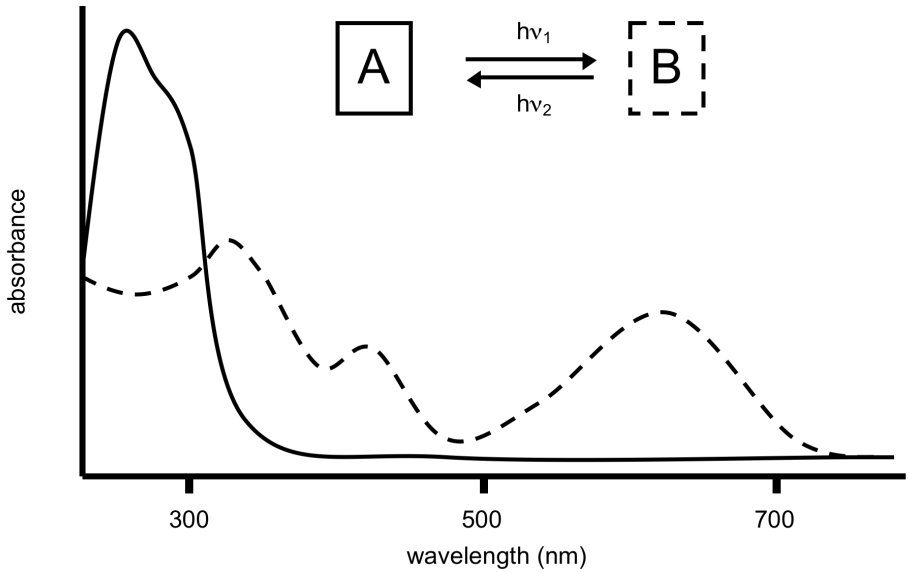

Figure 1.9 Hypothetical UV-Vis spectrum for the conversion of A to B. Exposure of A to light of photon energy $h\nu_1$ induces an isomerization to form B. B can be regenerated upon exposure to $h\nu_2$. Each isomer has a distinct UV-Vis spectrum.

Upon irradiation of *A* with a light of a particular frequency the absorption band in the UV region decreases while the absorption band in the UV-visible region grows. As a result, many photochromic molecules change from a colourless form to a coloured form, while other changes include, but are not limited to, change in shape, electronic structure and optical properties.

Ideally, both forms *A* and *B* absorb in well separated regions on the spectrum; however, there is often overlap in their absorption spectra which results in the formation of a chemical equilibrium between the two isomers. This equilibrium is referred to as the photostationary state (PSS) and is defined by the following equation:

$$\mathrm{PSS}(\%) = \frac{\text{molecules of one photoisomer}}{\text{total molecules of all photoisomers}} \times 100$$

Equation 1.1 Formula for the photostationary state of a photochemical system.

1.2.2 Types of Photochromic Reactions

Two main classes of photochromic systems are *cis-trans* isomerizations and electrocyclic photocyclizations.

1.2.2.1 *Cis-Trans* Isomerization

Azobenzene is perhaps the most well studied molecule that undergoes *cis-trans* photoisomerization. Azobenzene normally exist in the *trans*-form (**1.14**), and the *cis*-form (**1.15**) cannot be made by normal chemical methods. The *trans* to *cis* isomerization of the N=N bond is a result of the absorption of UV light, as shown in *Equation 1.2*. The reverse reaction either occurs thermally or by irradiation with visible light, making azobenzenes undesirable for any application that requires stability of both isomers.[23] Furthermore, the two forms of azobenzene do not have well separated λ_{max}, which precludes the selective irradiation or detection one particular isomer.

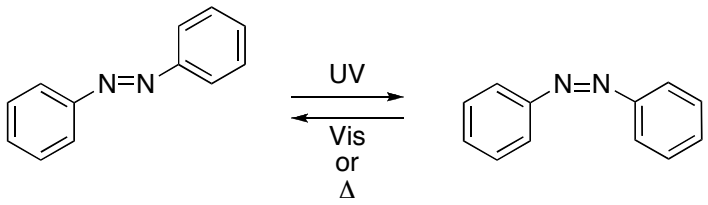

trans-isomer **1.14** *cis*-isomer **1.15**

Equation 1.2 Photoisomerization of azobenzene.

1.2.2.2 Electrocyclic ring cyclizations

Another class of photochromic molecules are those that undergo reversible ring opening/closing reactions. The most common molecules of this class are those containing 6π electrons arranged as a 1,3,5-hexatriene (**1.17**). As shown in *Equation 1.3*, upon

irradiation with the appropriate wavelength the molecule ring-closes and the ring-opening reactions occur with irradiation of different wavelengths.

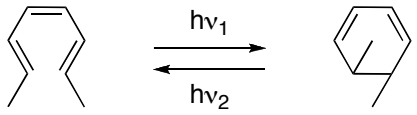

1,3,5-hexatriene **1.17** 1,3-cyclohexadiene **1.18**

Equation 1.3 Electrocyclization of 1,3,5-hexatriene upon irradiation with light of the appropriate wavelength.

Examples of 1,3,5-hexatriene systems are, fulgides (**1.18o**), spiropyrans (**1.19o**) and dithienylethenes (**1.20o**, **1.21o**), all of which undergo electrocyclization reactions (*Figure 1.10*). The ring-closing and ring-opening reactions of fulgides generate a significant number of side-products and spiropyrans can revert back thermally, however, dithienylethenes exhibit better photochemistry and excellent thermal stability at elevated temperatures (> 60 °C).[24,25]

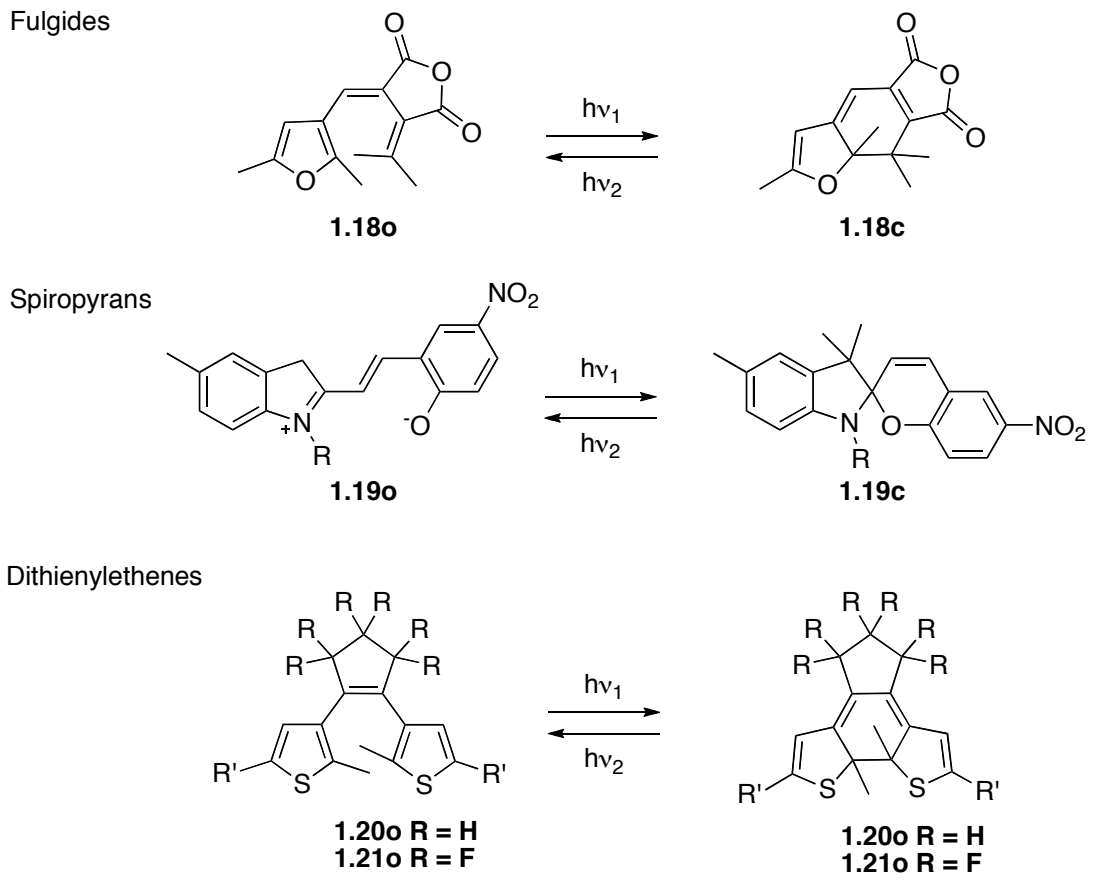

Figure 1.10 Three examples of common 1,3,5-hexatriene systems.

Since thermal stability is essential to the subject of this thesis, dithienylethenes (DTE's) were chosen to study, and their photochemistry will be discussed in detail below.

1.2.3 Photochemistry of dithienylethenes

The photoisomerization of dithienylethenes occurs *via* a conrotatory ring-closing reaction of the photoexcited ring-open form; however, the ring-open form can exist in a parallel or anti-parallel form and only the *anti*-parallel form will ring-close (*Figure 1.11).*[26]

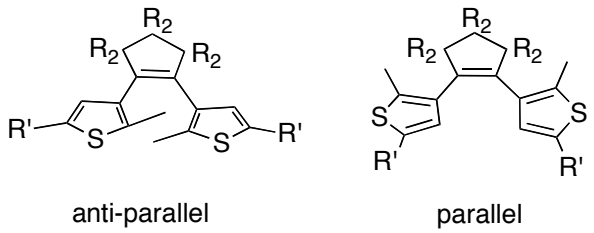

Figure 1.11 Parallel and *anti*-parallel forms of DTE. Ring closure only occurs for the anti-parallel form.

The molecular orbital diagram of 1,3,5 hexatriene is shown below in *Figure 1.12*, which is a simplified framework for dithienylethenes. Upon photoexcitation, an electron is promoted from the HOMO to the LUMO. Ring-closure occurs in a conrotatory manner in order to conserve π orbital symmetry. Only the anti-parallel form ring-closes as the ring-closing of the parallel form would require the interior methyl groups of the thiophene to overlap during the ring-closing process.

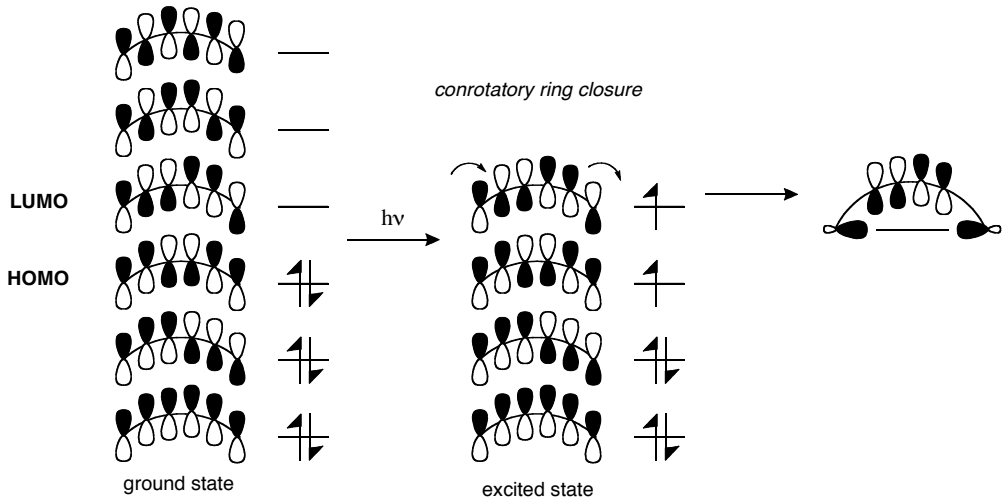

Figure 1.12 Frontier molecular orbital representation of the electrocyclic ring-closing reaction for the antiparallel form of a 1,3,5-hexatriene system.

As previously mentioned, the dithienylethenes have very good thermal stability, and they do not undergo thermal reversion to their ring open form. One of the key factors

affecting the stability of the ring-closed form is the type of heterocycle that is attached to the cyclopentene portion of the DTE. Upon ring closure, the resonance stabilization energy of the heterocycle is lost; this is the driving force for the thermally promoted ring-opening reaction. For example, diarylalkenes of pyrroles are thermally unstable since pyrroles have a high aromatic resonance stabilization energy. However, when thiophenes are used they have much greater thermal stability (> 3 months at 80 °C) owing to the low resonance stabilization energy of the thiophene rings.[21]

One of the major benefits of diarylethenes is their ability to be synthetically modified while retaining their photochemical properties. Two common strategies for making derivatives are to modify the DTE after the synthesis of the hexatriene backbone, or to functionalize the thiophene groups prior to the assembly of the photochromic molecule. The most common sites for synthetic modification are the thiophene C-5 and C-2 positions, which are shown below in *Figure 1.13*.[21,27]

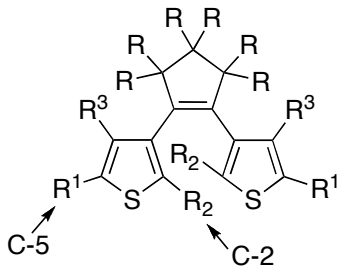

Figure 1.13 Common synthetic modification sites of DTE are “external” (C-5) or “internal” (C-2).

Peters *et al*. have shown that one of the thiophene rings can be replaced by a substituted olefin (*Figure 1.14*), which provides greater synthetic variability while retaining all the photochromic properties of DTE’s.[28]

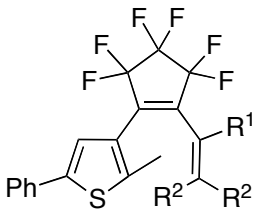

1.22o R^1R^2 = Ph
1.23o R^1 = CH_3 R^2 = Ph

Figure 1.14 Photochromic compounds based on a mono-thienylcyclopentene backbone allow for more synthetic variability, while retaining all the photochromic properties of DTE's.

Wustenberg *et al*. have further modified this structure by adding nitrile groups to the olefin, thus creating a dicyanoethylene-thienylethene (DCTE), as shown in *Figure 1.15*.[29, 30]

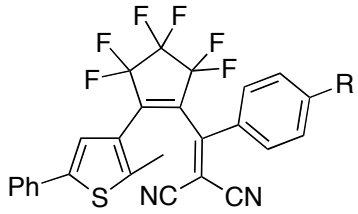

1.24o R = NO_2
1.25o R = H
1.26o R = OMe

Figure 1.15 Previously synthesized dicyanoethylene-thienylethene derivatives.[29, 30]

This architecture was of particular interest with respect to Karstedt's catalyst, as mentioned, electron deficient alkenes are known to inhibit the catalyst (see *Section 1.1.6*). As *Figure 1.16* illustrates, in the open form the DCTE has an electron deficient alkene (**1.24o**) that may inhibit the catalyst, and upon ring-closure (**1.24c**) the rearrangement of the π-system results in the loss of the coordination site. It should be noted phenyl or

alkyl-phenyl rings do not interact with the Karstedt's catalyst, which is supplied as a xylenes solution.

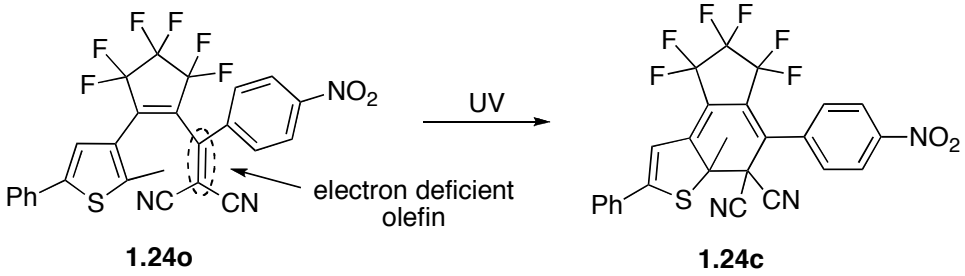

Figure 1.16 Ring closure of the DCTE results in the loss of an electron deficient double bond. In the open form the electron deficient double-bond is available for coordination to the catalyst while in the closed form this is not possible.

As shown in *Figure 1.17*, the DCTE would be added to the catalyst at room temperature, to displace the bridging siloxane ligand (**1.5**) and form the Karstedt-DCTE complex (**1.28**). At this point, the DCTE is blocking the coordination site and the catalyst is inhibited. Upon irradiation with the appropriate wavelength of light the DCTE undergoes ring-closure and consequently, loss of the coordination site. Thus, the cyclized DCTE (**1.24c**) is released and the active Karstedt catalyst (**1.7**) is generated.

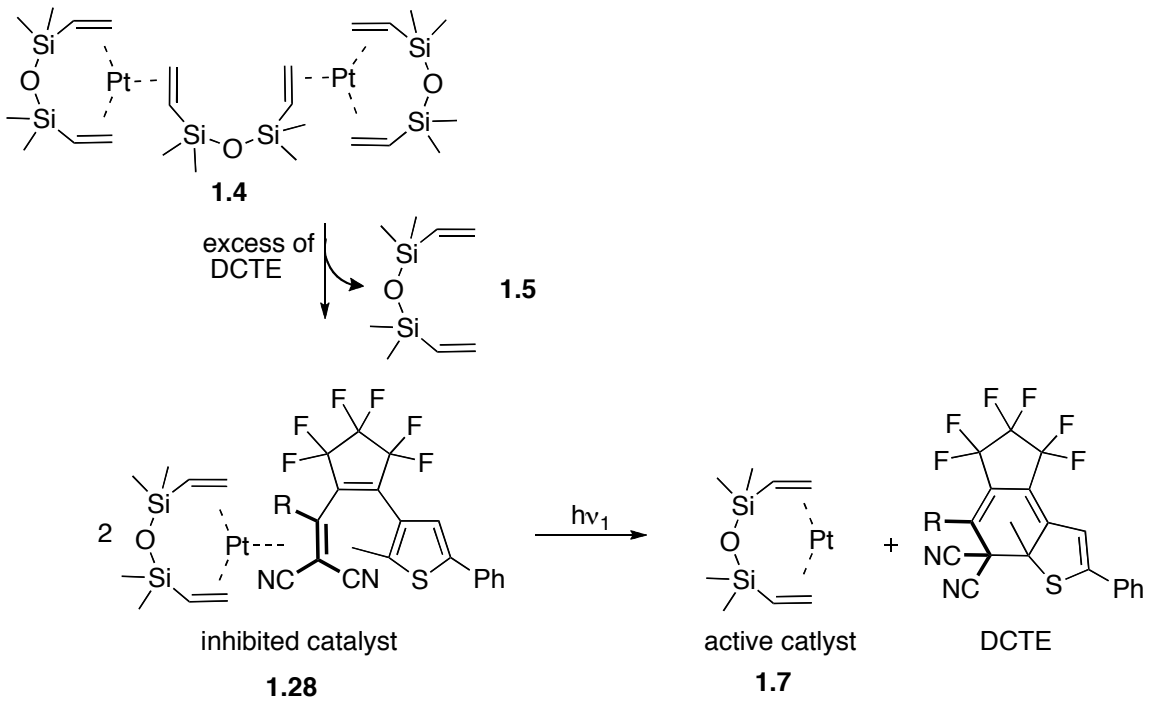

Figure 1.17 Proposed inhibition of Karstedt's catalyst by DCTE, and activation of the catalyst upon exposure to UV light.

This system would have many advantages over current protocols for the activation of Krastedt's catalyst, including the benefit of using light over heat, which was outlined in *Section 1.1.7*. Also, radiation-cured systems have higher turnover, less safety concerns and are more energy efficient. If successful, the system proposed herein, would, not only improve on a heat-cured system but also on the radiation-cured systems.

As the name implies, radiation-cured systems require radiation for the entire curing process. However, the method proposed in this thesis is a radiation-triggered system, thus the coated substrate needs only to be irradiated long enough to deactivate the inhibitor. Furthermore, the radiation acts directly on the catalyst, therefore, the range of reactants is no longer limited to those that contain photoactive functional groups. Finally, the choice of inhibitors is not restricted to those of intermediate strength. As discussed in

Section 1.13, the need for longer bath lives must be weighed against the need for low initiation temperatures. With the system proposed herein this is no longer an issue, as ligands that coordinate very strongly but effectively poison the catalyst could be used since the inhibitor looses the alkene coordination site in the ring-closed form. *Table 1.2* below summarizes the potential advantages of the proposed system.

Table 1.2 Summary of the advantages of using a radiation initiated system.

Improvement	Consequence
UV vs Heat	energy efficient shorter production time compact equipment fewer safety concerns
Radiation-Initiated vs Radiation-Cure	shorter radiation time
Targeting inhibitor over functional groups	wider application better "on" "off" control

2 EVALUATING THE INHIBITION OF KARSTEDT'S CATALYST BY WAY OF A HYDROSILYLATION REACTION

In this chapter the inhibition of Karstedt's catalyst is investigated by monitoring a typical hydrosilylation reaction. A series of model compounds based on the dicyanothienylethene (DCTE) architecture are synthesized and their inhibition ability towards the catalyst is assessed. A DCTE is chosen based on the model inhibitor experiments and synthesized. Although the DCTE was not a Karstedt's catalyst inhibitor, invaluable information regarding the development of a reliable and reproducible method for determining the inhibition ability of a ligand on Karstedt's catalyst is presented.

2.1 Introduction

2.1.1 Electron deficient olefins as Karstedt's catalyst inhibitors

Figure 2.1 shows some examples of electron deficient olefins which are known to inhibit Karstedt's catalyst.[19]

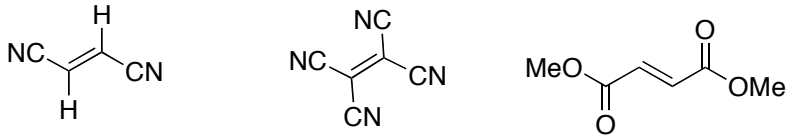

fumaronitrile **2.1** | tetracyanoethylene **2.2** | dimethyl fumarate **2.3**

Figure 2.1 Examples of Karstedt's catalyst inhibitors, which all contain electron deficient olefins.

The DCTE shown in *Figure 2.2* also possesses an electron deficient alkene. It is expected that the open-form of the DCTE will inhibit Karstedt's catalyst as it contains an electron deficient olefin, unlike the closed form which should not inhibit this catalyst.

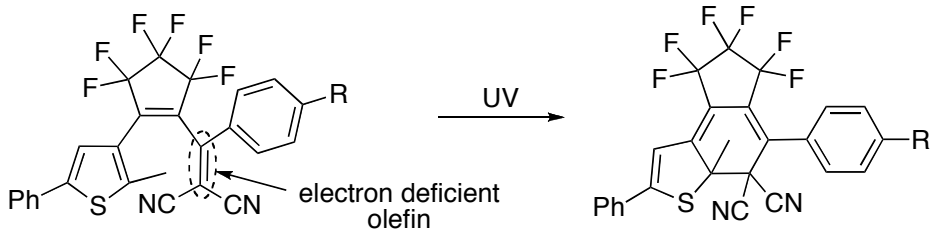

1.24o R = NO_2
1.25o R = H
1.26o R = OMe

1.24o R = NO_2
1.25o R = H
1.26o R = OMe

Figure 2.2 Examples of DCTE's containing an electron deficient alkene.

When designing a photoswitchable inhibitor for Karstedt's catalyst the photostationary state (PSS) of the inhibitor must be taken into account. Ideally, the molecule will have a PSS of 100%, and after irradiation there will be no ring-open form to inhibit the catalyst. A molecule with a PSS of less than 100% may also be useful, however the leftover ring-open form must not inhibit the catalyst significantly. Thus the required PSS for an effective photoswitchable inhibitor will depend on the strength of the inhibitor and will be different for any given molecule.

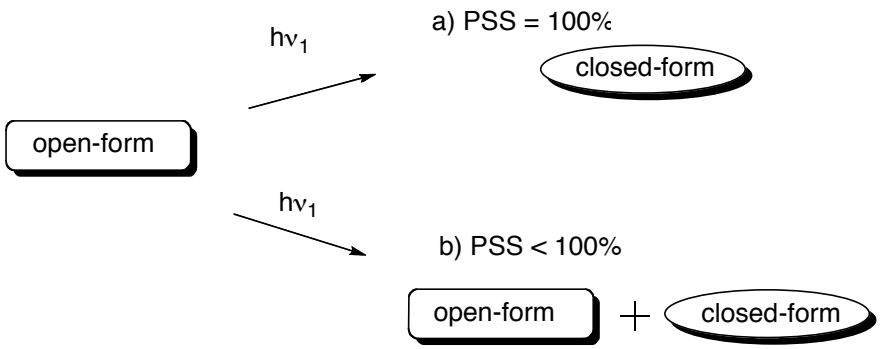

Equation 2.1 Difference between molecules with PSS = 100% and those with PSS < 100%.

2.1.2 Model inhibitors for preliminary studies

Synthesis of DCTE's usually involve six to eight synthetic steps; for that reason, it is more practical to synthesize model compounds based on the DCTE architecture to probe their ability to inhibit Karstedt's catalyst before synthesizing the complete DCTE.[29]

A series of model compounds **2.4**, **2.5**, **2.6** (*Figure 2.3)* were synthesized. These particular derivatives were chosen for the electron-donating or electron-withdrawing ability of the para-substituted functional group. If all the model compounds inhibited the catalyst, then the para-substituted functional group would not effect the degree of inhibition, indicating the dicyanoethylene moiety is sufficient for inhibition and that any of the proposed DCTE's can be chosen. However, if the para-substituted group does effect inhibition then only the DCTE based on the best model inhibitor should be pursued.

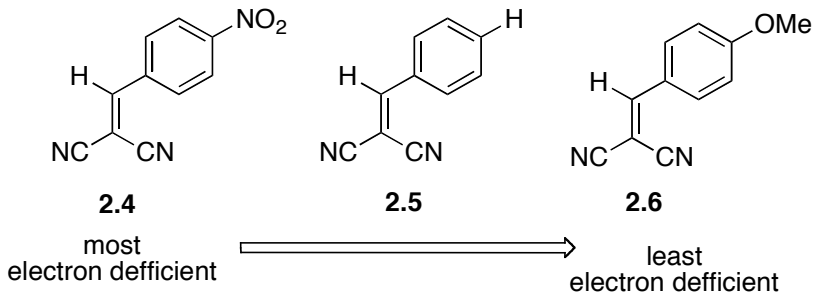

Figure 2.3 Design of model inhibitors based on the DCTE architecture. Each contain different para-substituted functional groups with varying electron donating/withdrawing capacities.

2.1.3 Testing for inhibition

The inhibition of Karstedt's catalyst is typically assessed by monitoring a test hydrosilylation reaction.[17,18,19] One of these hydrosilylation reactions is shown in *Equation 2.2*, which involves the reaction of vinyltrimethylsilane with a triethylsilane to produce triethyl(2-(trimethylsilyl)ethyl)silane. The vinyl-functionalized reagent is often used in excess to prevent the formation of platinum colloid species, which are known to cause unpredictable kinetic behaviour.[9]

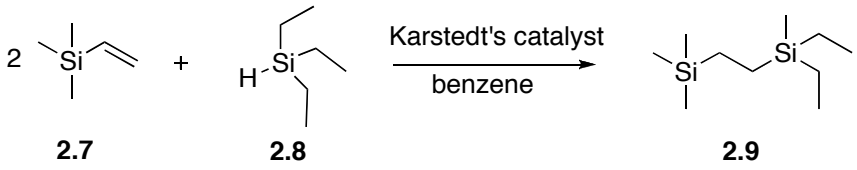

Equation 2.2 A simple hydrosilylation reaction involving vinyltrimethylsilane and triethylsilane to evaluate inhibition of Karstedt's catalyst.

The formation of **2.9** can be monitored by ^{1}H NMR spectroscopy or by gas chromatography (GC). Both methods have advantages and disadvantages; ^{1}H NMR spectroscopy is "ready to use" in that an experimental protocol does not need to be developed. The proton resonances of the product can readily be monitored; on the other

hand, the turn around time for sample measurements is limited by the number of scans needed for an appropriate signal to noise ratio. Furthermore, ^{1}H NMR spectroscopy has some upper concentration limits in order for the instrument to lock on the solvent signal. Gas chromatography does not have the same concentration limitations as ^{1}H NMR spectroscopy and the turn around time for sample measurements is shorter. However, an experimental protocol must be developed in order to insure proper resolution of peaks as well as linear response for peak area to product concentration. Although both methods are valid, gas chromatography is more versatile and is used more often.[17,18,19] *Figure 2.4* shows a typical ^{1}H NMR spectrum for the purified hydrosilylation product, and *Figure 2.5* shows typical GC chromatograph for the crude hydrosilylation reaction.

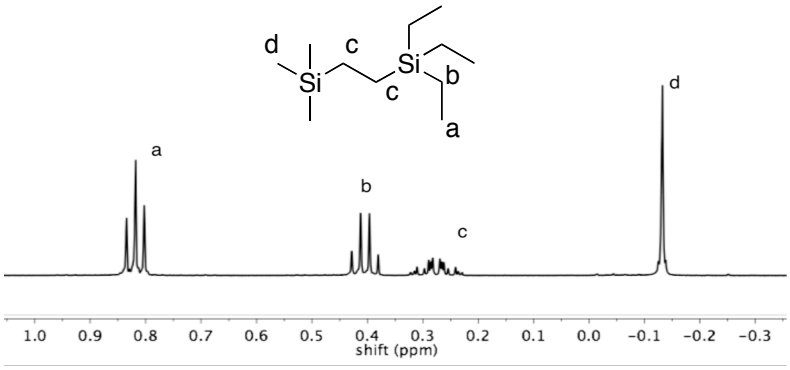

Figure 2.4 ^{1}H NMR spectra for hydrosilylation product **2.9**, after purification.

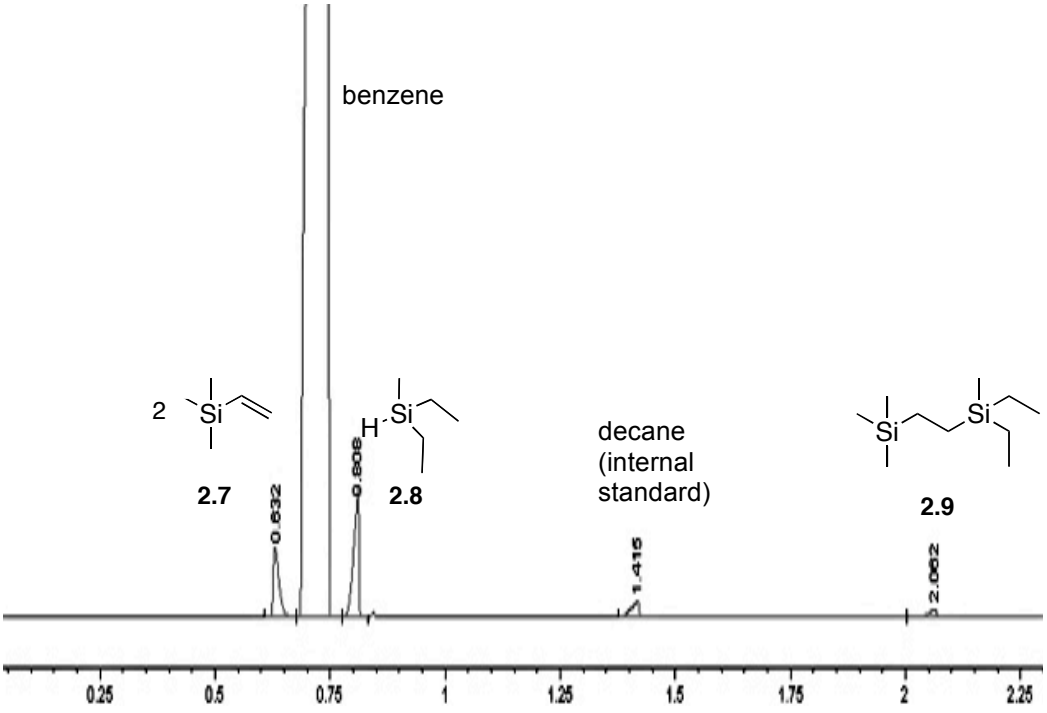

Figure 2.5 Typical GC chromatogram for crude hydrosilylation reaction, peaks shown (from left to right): vinyltrimethylsilane, benzene, triethylsilane, decane, product.

The proposed experiment for evaluating inhibition by certain ligands is shown in *Scheme 2.1*. This process is initiated by adding each proposed inhibitor (35 equivalents) to a solution of Karstedt's catalyst and incubating for one hour at 50 °C, after which the reactants are added and the reaction progress is monitored. These conditions were chosen based on previous Karstedt catalyst inhibition studies.[17]

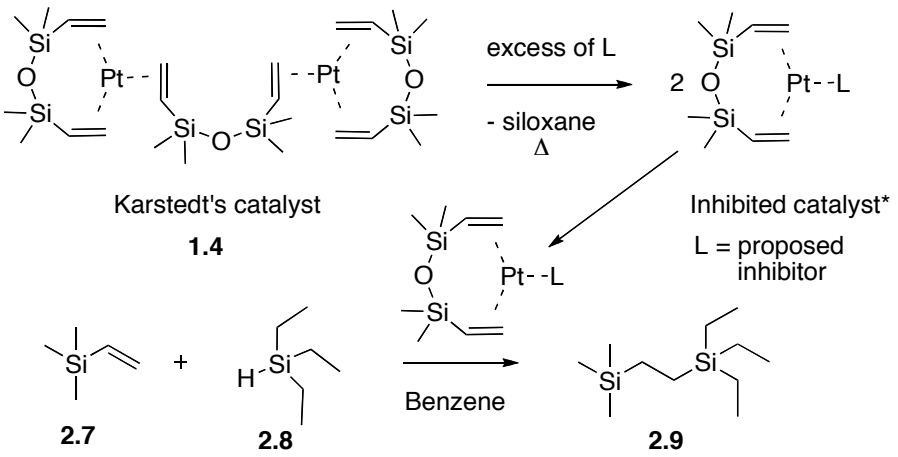

Scheme 2.1 Proposed method for evaluating the inhibition of Karstedt's catalyst.*Predicted complex based on previous inhibited Karstedt catalyst structures.

2.1.3.1 Molar equivalents and concentration of reagents

The limiting reagent in a hydrosilylation reaction can effect which mechanism the reaction proceeds through. For example, if the silane molecule is used in excess, then platinum colloids can form, which greatly effects the kinetics of the reaction. Consequently, the reagent ratios must be identical for each reaction, which will ensure that any observed rate difference between two inhibitors is not a result of differing reagent ratios. The best way of ensuring identical reagents ratios is by preparing stock solutions of reagents and adding them directly to the catalyst solution.

2.1.3.2 Karstedt's catalyst medium

Two forms of Karstedt's catalyst can be purchased: 1) as a solution in divinyltetramethyldisiloxane (DVTMS) and 2) as a solution in xylenes. The major advantage of purchasing the catalyst in a DVTMS solution is that the catalyst is more stable; however the catalyst is more difficult to handle as the catalyst in the DVTMS solution is extremely viscous, rendering its measurement tedious. Therefore if small

quantities of catalyst are needed (<10 μL) Karstedt's catalyst in a solution of DVTMS is not practical.

While the Karstedt's catalyst xylenes solution is much easier to handle and small quantities (<10 μL) can be readily measured, the catalyst-xylenes solution is less stable and also needs to be replaced more frequently than the catalyst in DVTMS solution.

Karstedt's catalyst can also be synthesized directly from chloroplatinic acid (H_2PtCl_6) and DVTMS. This reaction was attempted numerous times, however, none of the attempts were successful. Since Karstedt's catalyst could be readily purchased from Aldrich (as well as other chemical suppliers) this approach was abandoned.

The solubility of the desired ligand (or inhibitor) must also be taken into account when choosing the medium of Karstedt's catalyst. Karstedt catalyst can form colloidal species, which are aggregates of the mononuclear platinum complex. Although a ligand may be soluble in the solvent, it may not be able to diffuse through such a colloidal sphere. Inhibited Karstedt's catalyst complexes can also form colloidal species, where the inhibited complex forms a insoluble colloid. In this case, the colloid prevents reagents from diffusing through and having contact with the platinum, thus the inhibition mechanism is more complicated than simple crowding of the coordination site. This phenomenon can be influenced by the choice of catalyst medium. Colloidal species will form when the mononuclear complex is not stable, therefore colloidal species should be less likely to form when the more stable catalyst solution is used (DVTMS). Both methods of inhibition are equally valuable, however, the formation of colloids can lead to different kinetic behaviour than the mononuclear species. Thus, an experimental protocol

to test both catalyst media was developed, as it is possible that the different media can lead to different inhibition mechanisms.

2.2 Results and discussion

2.2.1 Synthesis of model compounds

Compounds **2.4**, **2.5**, and **2.6** were all synthesized from the corresponding commercially available aldehyde (**2.13**, **2.14**, **2.15**) by performing Knoevenagel condensations (*Equation 2.3*), which involved treating the aldehyde with malononitrile and a catalytic amount of piperidine. The suspension was heated to reflux, and upon cooling the product (**2.4**, **2.5**, **2.6**) precipitated and was isolated by vacuum filtration. The structure of the product was confirmed by the disappearance of the aldehyde resonance in (δ = 10 ppm) and the presence of a new resonance (δ = 7-8 ppm) in the ^{1}H NMR spectrum, that was attributed to the dicyanoethylene proton.

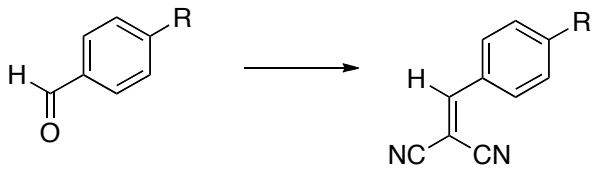

2.10 R = NO_2
2.11 R = H
2.12 R = OMe

2.4 R = NO_2
2.5 R = H
2.6 R = OMe

Equation 2.3 Preparation of model compounds **2.4**, **2.5**, and **2.6** by way of a Knoevenagel condensation reaction. Reaction conditions: malononitrile, piperidine, EtOH, reflux.

2.2.2 Synthesis of DCTE

The DCTE synthesis was carried out as previously reported (*Scheme 2.2*).[30]

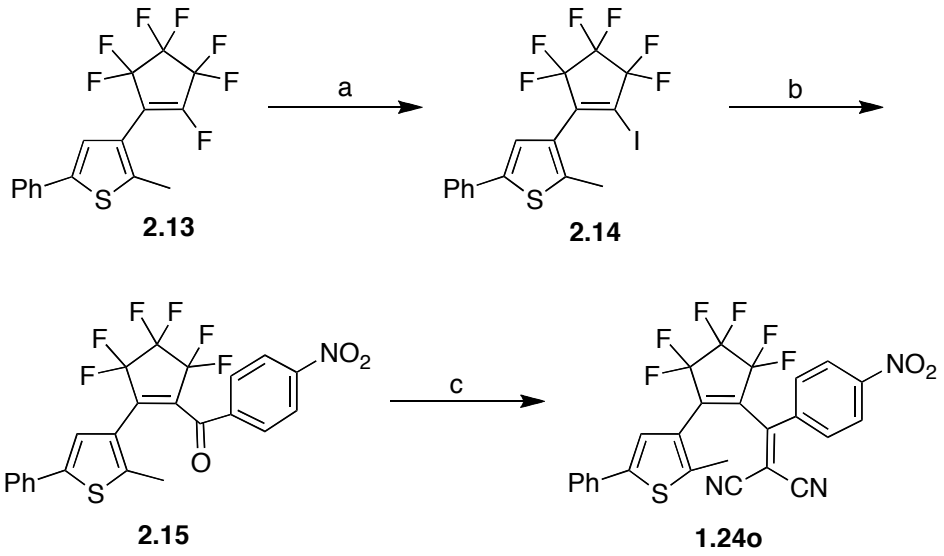

Scheme 2.2 Synthesis of DCTE as previously reported. Reaction conditions: a) NaI, DMF, 145 °C, 18%; b) 1. *n*-BuLi, 2) 4-nitrobenzoyl chloride, Et_2O, -78 °C, 65%; c) malononitrile, $TiCl_4$, pyridine, DCE, reflux, 60%.

Preparation of **1.24o** began with the treatment of 2-methyl-3-(perfluorocyclopent-1-enyl)-5-phenylthiophene (**2.13**)[30] with sodium iodide in DMF at 140 °C to produce 3-(3,3,4,4,5,5-hexafluoro-2-iodocyclopent-1-enyl)-2-methy1-5-phenylthiophene (**2.14)** in 18% yield. The structure was confirmed by the shifting upfield of the thiophene proton resonance in the ^{1}H NMR spectrum, unreacted starting material **2.13** can be recovered almost quantitatively. The anion formed from the treatment of **2.14** with *n*-BuLi is then reacted with the appropriate acyl chloride to generate 3,3,4,4,5,5-hexafluoro-2-(2-methyl-5-phenylthiophen-3-yl)cyclopent-1-enyl)(4-nitrophenyl)methanone (**2.15)** in 65% yield, as confirmed by the four line pattern of the new phenyl protons in the ^{1}H NMR spectrum. The aldehyde **2.15** is then reacted with malonitrile to afford the DCTE **1.24o** in 60% yield.[30]

2.2.3 Inhibition of Karstedt's catalyst as observed by ^{1}H NMR spectroscopy

2.2.3.1 Inhibition by model compounds

The inhibition of Karstedt's catalyst by model inhibitors was evaluated by ^{1}H NMR spectroscopy. The results of the experiments are outlined below in *Table 2.1*. This experiment involved four molecules: **2.4**, **2.5**, **2.6**, and a known inhibitor (**2.3**) which were incubated with Karstedt's catalyst for 1 hour at 50 °C. A solution of starting materials (**2.7** and **2.8**) was then added. The solutions were allowed to react for one hour, after which ^{1}H NMR spectra were taken. Percent completion was calculated as shown in *Equation 2.4*.

Table 2.1 Results for the inhibition of Karstedt's catalyst by evaluation of a hydrosilylation reaction between **2.7** and **2.8** to form **2.9** with inhibitors **2.4**, **2.5**, **2.6**.

Molecule	% Completion
2.3	11
2.4	33
2.5	85
2.6	95
control (no inhibitor)	98

Reaction conditions: Karstedt's catalyst (1×10^{-4} mmol) was incubated with 3.5×10^{-3} mmol of **2.4**, 3.2×10^{-3} mmol of **2.5** and 3.8×10^{-3} mmol of **2.6** for 1 h then reacted with 0.01 mmol of **2.7** and 0.005 mmol of **2.8** at room temperature.

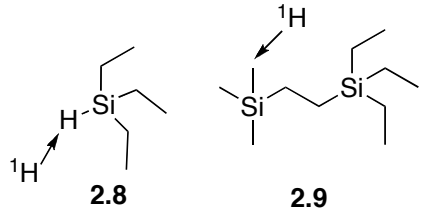

2.8 **2.9**

$$\%\,Completion = \frac{\text{product integration (}\mathbf{2.9}\text{)}}{\text{product integration (}\mathbf{2.9}\text{) + silane integration (}\mathbf{2.8}\text{)}} \times 100\%$$

Equation 2.4 Percent completion formulation as determined by ^{1}H NMR integration.

2.2.3.2 Inhibition by DCTE

The same hydrosilylation reaction was used to evaluate the inhibition of Karstedt's catalyst by compound **1.24o** and compound **1.24c**. The study involved three simultaneous reactions as shown in *Scheme 2.3*: 1) a control with no inhibitor, 2) with inhibitor **1.24o,** and 3) and with inhibitor **1.24o** (to be irradiated). These solution were added to Karstedt's catalyst and incubated at 50 °C for 1 hour after which reagents **2.7** and **2.8** were added. The reaction progress was then monitored by ^{1}H NMR spectroscopy. After 30 minutes, one of the **1.24o** solutions was irradiated to generate **1.24c** and the reaction progress was monitored. The study showed a noticeable difference between the inhibition abilities of **1.24o** and **1.24c** (*Figure 2.6*).

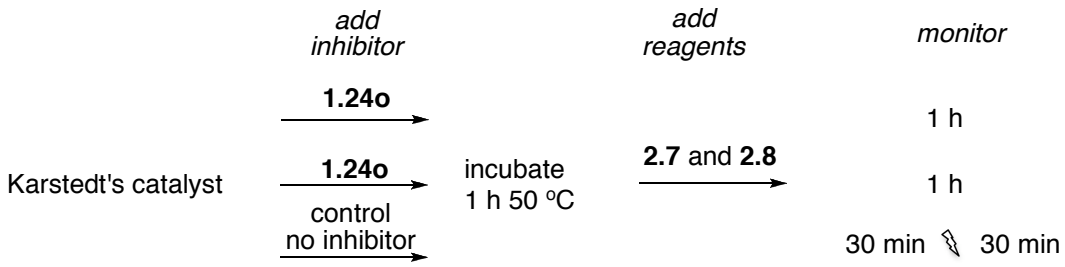

Scheme 2.3 Experimental set up for the study of the inhibition of Karstedt's catalyst by **1.24o** compared to **1.24c**.

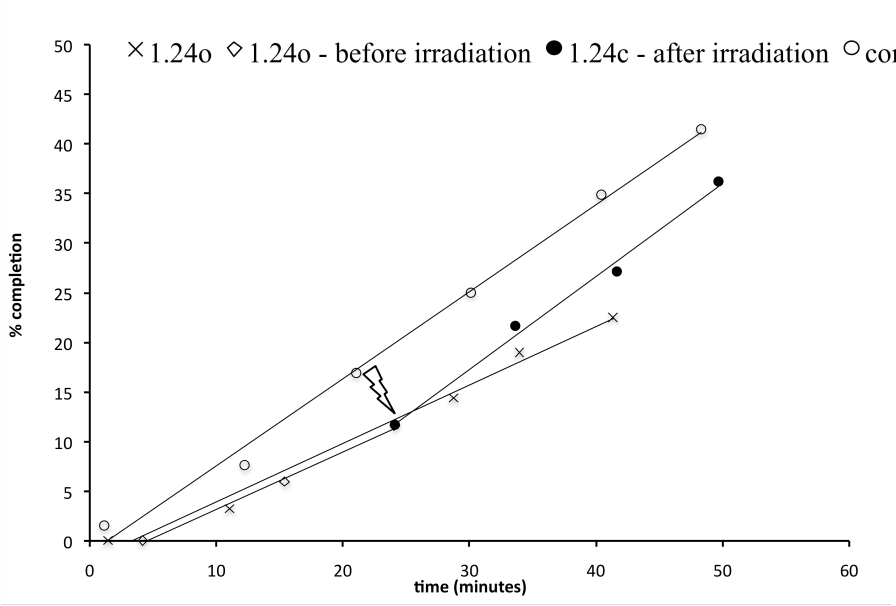

Figure 2.6 Percent completion versus time for the determination of difference in the inhibition ability between **1.24o** and **1.24c** on Karstedt's catalyst by monitoring a test hydrosilylation reaction. Reaction conditions: Two solutions of Karstedt's catalyst (0.14 μmol) were incubated with **1.24o** (4.5 μmol) for 1 h then reacted with **2.7** (0.012 mmol) and **2.8** (0.006 mmol) at room temperature. After 30 one of the solutions was irradiated with 313 nm light for 9 min. Relative error in measurement is ~ ± 5%. min

Although the above data suggests there is a slight difference in the inhibiting ability of **1.24o** compared to **1.24c,** the difference is still within experimental error or may be attributed to the induction period for Karstedt's catalyst, which will be discussed further in *Section 2.2.3.1*. Several attempts were made at replicating the results shown in *Figure 2.6*. However, several problems were encountered during the repetition of this process. Frequently, the catalyst simply did not catalyze the reaction. Other times, the reaction would finish so quickly it could not be monitored. Reasons for this inconsistency will be further speculated in this chapter. As a result, a more reliable and reproducible method was needed. For several practical reasons that will be discussed in *Section 2.2.3.2*, ^{1}H NMR spectroscopy was abandoned as a method for evaluating the hydrosilylation reaction and instead, gas chromatography was used.

2.2.3.1 Induction period for Karstedt's catalyst

In some of the reaction graphs, an example of which is shown in *Figure 2.7*, an initial upward curve was observed. This behaviour is not uncommon for Karstedt-catalyzed hydrosilylation reactions.

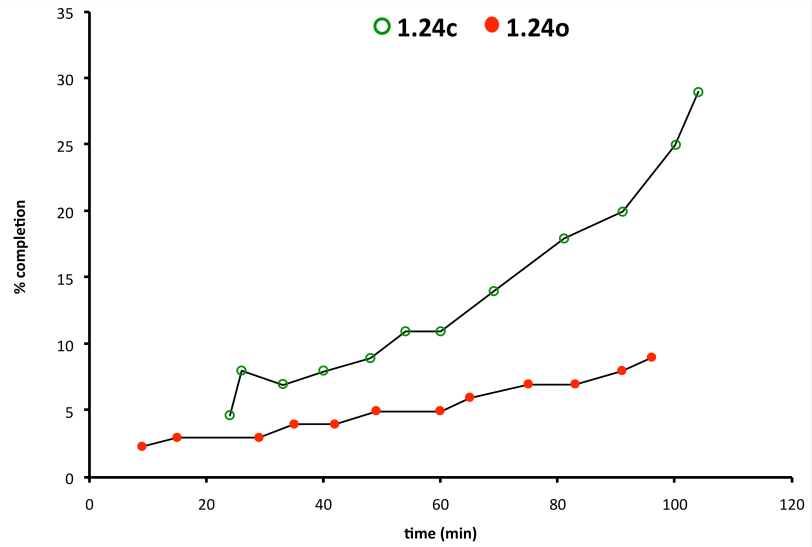

Figure 2.7 Percent completion versus time for the determination of difference in the inhibition ability between 1.24o and 1.24c on Karstedt's catalyst showing the initial upwards slope which is attributed to the induction period.

This phenomenon is often referred to as an induction period or a "slow" reaction period since some hydrosilylation product is formed.[9] The rational for this observed induction period is illustrated below in *Scheme 2.4*. Before the hydrosilylation of the added olefin can occur, the vinyl groups of the bound ligand (DVTMS in this case) must first undergo hydrosilylation, after which the added olefin can be hydrosilylated. This has been shown not only with bound DVTMS ligands, but also in other Karstedt complexes containing ligands with alkene groups.[31] Generally speaking, stronger coordinating alkenes are hydrosilylated at a faster rate; in the case of DVTMS and vinyltrimethylsilane, the bound DVTMS will react faster than the added olefin

(vinyltrimethylsilane) and therefore an induction period is observed. However, some vinyltrimethylsilane will react as a result of ligand exchange, but this exchange is slow, resulting in only a small amount of product being made during the induction period.

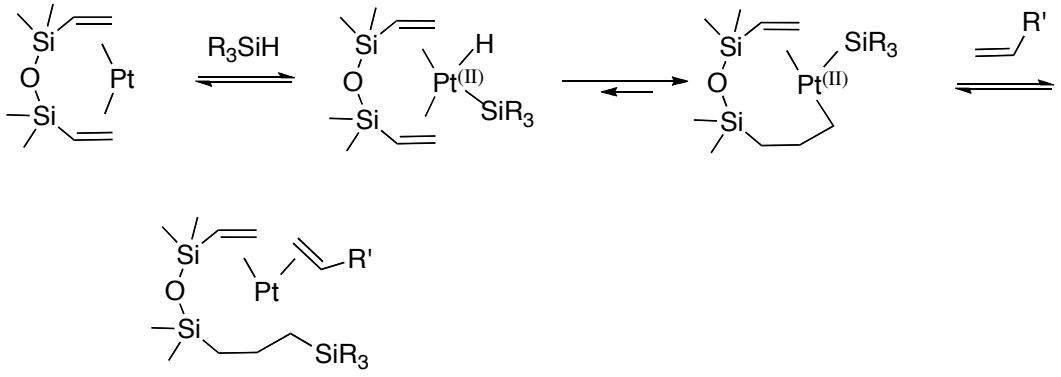

Scheme 2.4 Reaction occurring during the induction period for Karstedt's catalyst. For triethylsilane R = Et, and R' = $Si(Me)_3$ for vinyltrimethylsilane.

It is important to take into account this induction period when evaluating reaction kinetics for this hydrosilylation reaction. As shown in *Figure 2.7,* different reactions may have different induction periods which can be confusing when trying to determine a rate difference. Upon first glance at the data, it appears as though the reaction containing the open-form of the DCTE is being inhibited compared to the reaction containing the closed-form of the DCTE; however after repeating this experiment it was found that this was not the case and it is likely that this apparent difference in rate is in fact due to a difference in induction periods. In order to minimize any error in interpretation of data due to the induction period, it is important to follow all reactions to completion as the initial rates can not be used to determine rate differences. Also to be noted, heating the reaction slightly can shorten the induction period.

2.2.3.2 Problems with ^{1}H NMR as an a method for evaluating catalyst inhibition

Bearing the results discussed above in mind, a more robust method was needed. Consequently, several variables of the hydrosilylation reaction needed to be changed and ^{1}H NMR spectroscopy did not lend itself well to this process. As previously mentioned, ^{1}H NMR spectroscopy has concentration limits which GC does not. Furthermore, purification of deuterated benzene required for the reaction solvent was uneconomical and more time consuming compared to GC monitored reactions where benzene from a solvent purification system could be used. Finally, temperature control of the reaction, is more difficult when using NMR spectroscopy to monitor reaction progress. For all of these reasons, ^{1}H NMR spectroscopy was abandoned as a detection method and gas chromatography was employed.

2.2.4 Inhibition of Karstedt's catalyst as observed by gas chromatography

The development of a method to evaluate the inhibition of Karstedt's catalyst proved to be much more problematic than originally anticipated. However, after considerable effort, GC was found to be a more reliable and reproducible method of evaluating the hydrosilylation reactions.

2.2.4.1 Temperature effects

Like all reactions, the Karstedt-catalyzed hydrosilylation reaction is effected by temperature, and for the benefit of reproducibility, it is important that all reactions be performed at the same temperature. The ideal temperature to perform the reaction is dependent on the concentration of reagents and catalyst. For the purpose of these studies,

30 to 40 °C was identified as an ideal temperature to generate a reproducible reaction curve with a short induction period.

2.2.4.2 Inhibition by model compounds

The inhibition of Karstedt's catalyst by the model compounds **2.4** and **2.5** was also performed with the improved GC method and the result which had been previously obtained were confirmed. The experimental set up is shown in *Scheme 2.5* and the data obtained is plotted in *Figure 2.8*.

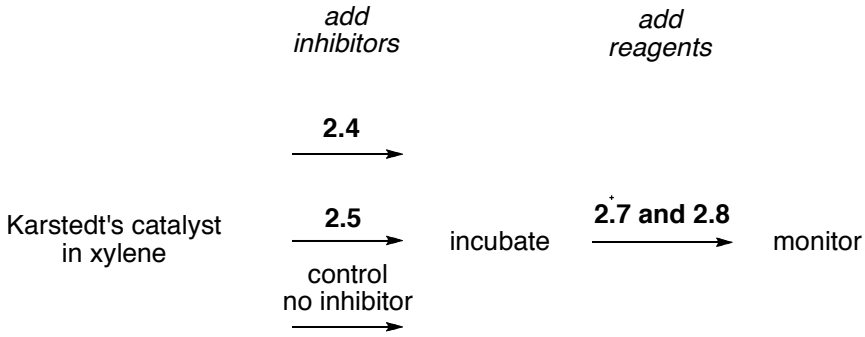

Scheme 2.5 Experimental set up for the inhibition of Karstedt's catalyst by **2.4** and **2.5.**

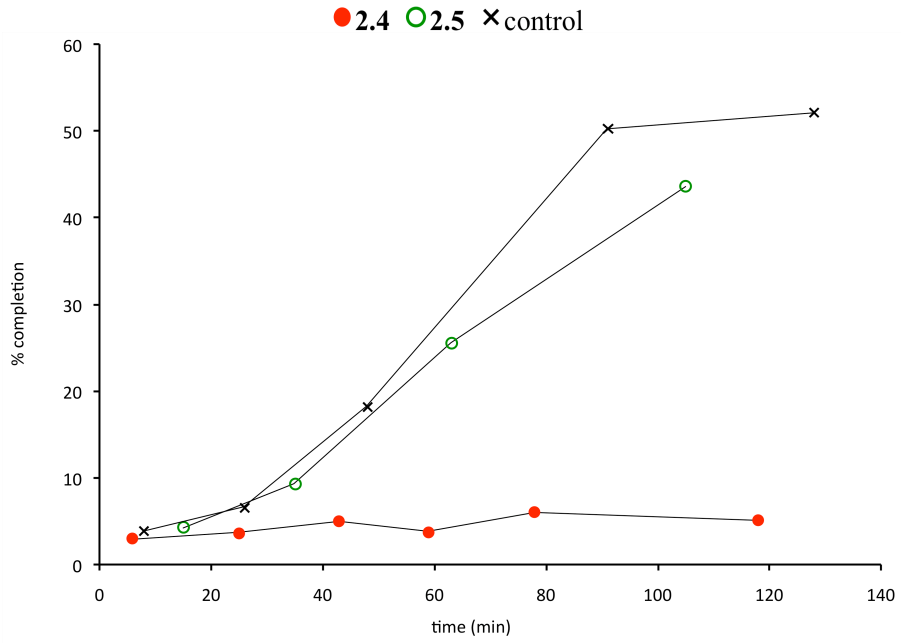

Figure 2.8 Percent completion versus time for the determination of the inhibition of Karstedt's catalyst by **2.4** and **2.5** by monitoring a hydrosilylation reaction. Reaction conditions: Karstedt's catalyst (0.5 mM) was incubated with **2.4** (16 mM) and with **2.5** (16 mM) for 1 h then reacted with **2.7** and **2.8** (0.44 M, 0.22 M). Relative error in measurement is ~ ± 5%.

As in the previous experiment, the nitro substituted model showed significant inhibition while the unsubstituted model showed no inhibition, which suggested that the dicyanoethylene portion of the molecule was not sufficient for inhibition.

2.2.4.3 Inhibition by DCTE

The experiment involved three simultaneous reactions: one containing **1.24o**, one containing a PSS solution of 1.24c and a control with no inhibitor (*Figure 2.9*).

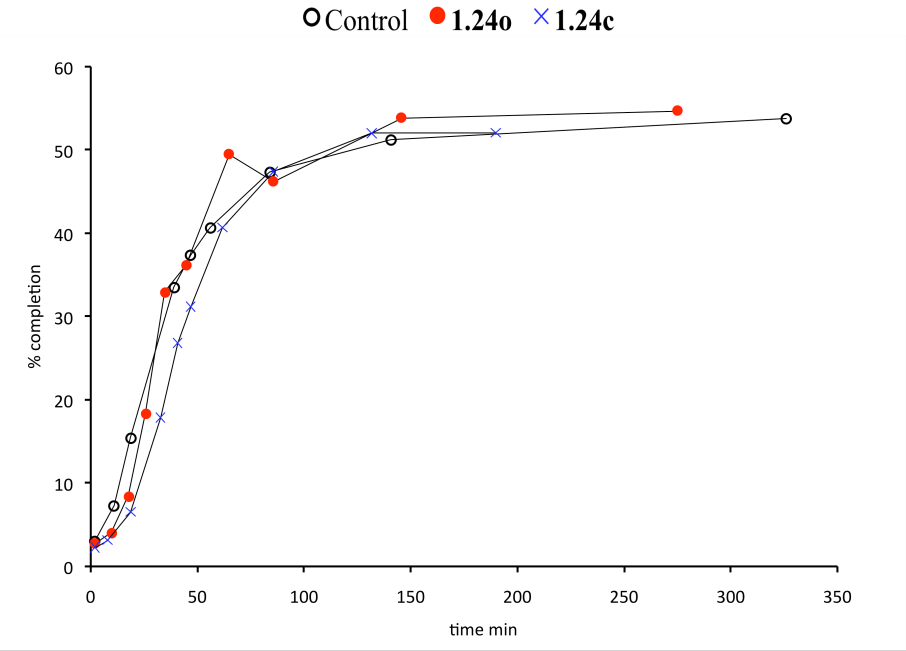

Figure 2.9 Percent completion versus time for the determination of difference in the inhibition ability between **1.24o** and **1.24c** on Karstedt's catalyst by monitoring a test hydrosilylation reaction. Reaction conditions: Karstedt's catalyst (0.47 mM) was incubated with **1.24o** (17 mM) and with **1.24c** (17 mM) for 1 h then reacted with **2.7** and **2.8** (0.46 M, 0.23 M). Relative error in measurement is ~ ± 5%.

The results of this experiment indicated no inhibition ability of either the open or closed form of the DCTE. It is possible that the previously observed rate difference was simply a result of different induction periods for each reaction. The lack of inhibition may be a result of steric bulk. This will be further discussed in the next section.

2.2.5 Effect of steric bulk

By comparing the coordination site of the model compound (**2.4**) with that of the DCTE (**1.24o**), the alkene of the DCTE should be more electron deficient as it is connected to the highly electron withdrawing hexafluorocyclopentene ring. Therefore it can be speculated that the lack of inhibition of the DCTE must be due to the additional steric bulk of the hexafluoro ring. Thus, any future photoswitchable Karstedt's catalyst

inhibitors based on a DCTE architecture will have to account for steric bulk around the dicyanoethylene coordination site.

2.2.6 Effect of catalyst medium

Finally, both catalyst solutions were used in separate experiments, and neither medium was shown to effect the inhibition of Karstedt's catalyst. No inhibiting difference between **1.24o** and **1.24c** was shown in either case, while the model inhibitor (**2.4**) was found to inhibit with either catalyst medium.

2.3 Conclusion

A series of model inhibitors based on the DCTE architecture were synthesized and tested for inhibition of Karstedt's catalyst. The dicyanoethylene moiety alone was found to be insufficient to inhibit the catalyst and only the nitro-substituted inhibitor was found to inhibit. Based on these results, DCTE **1.24o** was synthesized but was not found to be a Karstedt catalyst inhibitor, most likely as a result of the added steric bulk of the hexafluoro ring. More importantly, a reliable method for determining the inhibition of Karstedt's catalyst was developed and considerations for future experiments are outlined below.

1. All reactions should be followed to completion as initial rates can not be used as Karstedt's catalyst often undergoes an incubation period.
2. Identical reagent ratios must be used and therefore preparation of stock solutions is recommended.
3. Both Karstedt's catalyst solutions (DVTMS and xylenes) should be employed as they can lead to different inhibition mechanisms; if

microlitre quantities of catalyst are needed then only the xylenes solution can be accurately measured.

4. All reactions should be performed at the same temperature for the sake of reproducibility and this temperature will be dependant on catalyst and reagent calculations.

Although the experiments performed in this chapter provided good insight into the inhibition of Karstedt's catalyst, it was still an indirect method of assessing the interaction with the catalyst. Also, hydrosilylation reactions were time consuming and a quicker method for assessing a molecule's inhibition ability was needed. NMR spectroscopy is often used to assess the binding affinities of two compounds and could be used to assess an inhibitor's interaction with Karstedt's catalyst and therefore its potential inhibition ability. *Chapter 3* will focus on using ^{1}H NMR spectroscopy as a screening tool for inhibitors.

2.4 Experimental

2.4.1 Materials

All solvents for hydrosilylation reactions were dried and degassed by passing through steel columns containing activated alumina under nitrogen using an MBraun solvent purification system. Solvents for metal halogen exchange reactions were dried by refluxing over sodium. All other solvents were used as received. Column chromatography was performed using silica gel 60 (230-400 mesh) from Silicycle Inc., or with a Teledyne Isco CombiFlash Companion sg100c and redisep normal phase silica columns. Karstedt's catalyst and all other reagents and starting materials were purchased from Aldrich.

2.4.2 Techniques

^{1}H NMR spectroscopic characterizations were performed on a Varian Inova 500 instrument (499.8 MHz for ^{1}H NMR). Chemical shifts *(δ)* are reported in parts per million using the residual solvent signal as a reference standard: $CDCl_3$ (δ = 7.26 ppm), C_6D_6 (δ = 7.16 ppm). Coupling constants *(J)* are reported in Hertz. UV-VIS measurements were performed using a Varian Cary 300 Bio spectrophotometer. Melting point measurements were performed using a Fisher-Johns melting point apparatus. Gas chromatography (GC) was performed on a Agilent 6890N, Stationary Phase: HP-5 (30 m x 0.322 mm x 0.25 μm).

2.4.3 Photochemistry

Standard lamps used for visualizing TLC plates (Spectroline E-series, 470 mW/cm^2) were used to carry out all the ring-closing reactions. A 313 nm light source was used.

2.4.4 Synthesis of Model Compounds

2-(4-Nitrobenzylidene)malononitrile (**2.4**)

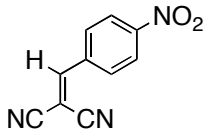

A solution of p-nitrobenzaldehyde (500 mg, 3.31 mmol) and malononitrile (220 mg, 3.31 mmol) were dissolved in refluxing ethanol (5 mL), at which point a catalytic amount of piperidine (1 drop) was added. The resulting dark red solution was heated for an additional 1 h. The solution was cooled to room temperature and then added to chilled distilled water (75 mL, 5 °C), after which a brown precipitate formed. The precipitate was collected by vacuum filtration and the product was washed with cold ethanol, yielding 2-(4-nitrobenzylidene)malononitrile (414 mg, 63%) as a brown solid. Mp = 160-161 °C (lit. 161.5-162 °C) [32]

^{1}H NMR (C_6D_6, 600 MHz): δ ppm = 7.91 (s, 1H), 7.77 (d, J = 8.8 Hz, 2H), 7.41 (d, J = 8.8 Hz, 2H).[33]

2-Benzylidenemalononitrile (**2.5**)

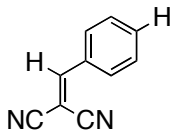

A solution of benzaldehyde (500 mg, 4.72 mmol) and malononitrile (331 mg, 4.72 mmol) were dissolved in refluxing ethanol (5 mL), at which point a catalytic amount of piperidine (1 drop) was added. After 1 h the solution was cooled to room temperature and added to cooled distilled water (75 mL, 5 °C). This solution was then concentrated to 30 mL and a pale yellow precipitate formed. The precipitate was collected by vacuum filtration and the product was washed with cold ethanol, yielding 2-benzylidenemalononitrile (500 mg, 69%) as a pale yellow solid. Mp = 81-82 °C (lit. 81.0-82.0 °C).[32]

^{1}H NMR (C_6D_6, 500 MHz): δ ppm =7.18 (t, J = 7.8 Hz, 2H), 6.84 (d, J = 7.4 Hz, 1H), 6.77 (t, J = 7.7, 2H), 6.41 (s, 1H).[33]

2-(4-Methoxybenzylidene)malononitrile (**2.6**)

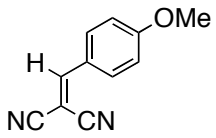

A solution of anisaldehyde (500 mg, 3.67 mmol) and malononitrile (240 mg, 3.67 mmol) were dissolved in refluxing ethanol (5 mL), at which point a catalytic amount of piperidine (1 drop) was added. After 1 h, the solution was cooled to room temperature

and a light yellow precipitate formed. The precipitate was collected by vacuum filtration and the product was washed with cold ethanol, yielding 507 mg of 2-(4-methoxybenzylidene)malononitrile (507 mg, 75%) as a yellow solid. Mp = 112-113 °C (lit. 113.5-114 °C).[32]

^{1}H NMR ($CDCl_3$, 500 MHz): δ ppm = 7.91 (d, J = 9 Hz 2H), 7.65 (s, 1H), 7.01(d, J = 9 Hz, 2H), 3.92 (s, 3H).[33]

2.4.5 Synthesis of DCTE

3-(3,3,4,4,5,5-Hexafluoro-2-iodocyclopent-1-enyl)-2-methyl-5-phenylthiophene (**2.13)**

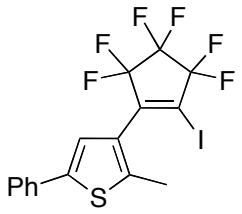

In a nitrogen flushed 100 mL Schlenk tube equipped with a magnetic stir bar 1-(2-methyl-5-phenyl-3-thienyl)perfluorocyclopent-1-ene (2.0 g, 5.5 mmol) and anhydrous sodium iodide (1.40 g, 11.9 mmol), followed by anhydrous DMF (10 mL) were added. The tube was sealed and the solution was heated at 145 °C in an oil bath for 6 h. The oil bath was turned off and the reaction was allowed to stir for an additional 18 h. To the reaction, water (50 mL) was added and the organic layer was extracted with Et_2O (3 × 75 mL). The combined organic layers were washed with water, brine, and dried over Na_2SO_4, filtered and evaporated to dryness under vacuum. Purification by column chromatography (SiO_2, hexanes) yielded 3-(3,3,4,4,5,5-hexafluoro-2-iodocyclopent-1-

enyl)-2-methyl-5-phenylthiophene (464 mg, 18%) as a white solid. Mp = 74-75 °C, (lit. 74 °C).[30]

^{1}H NMR ($CDCl_3$, 500 MHz): δ (ppm) =7.55 (t, J = 7 Hz, 2H), 7.39 (m, 2H), 7.31 (m, 1H), 7.10 (s, 1H), 2.46 (s, 3H).[30]

3,3,4,4,5,5-Hexafluoro-2-(2-methyl-5-phenylthiophen-3-yl)cyclopent-1-enyl)(4-nitrophenyl)methanone (**2.14**)

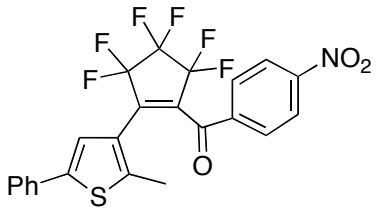

In a flame dried 10 mL round bottom flask, 3-(3,3,4,4,5,5-hexafluoro-2-iodocyclopent-1-enyl)-2-methyl-5-phenylthiophene (180 mg, 0.38 mmol) was dissolved in anhydrous Et_2O (5 mL). The solution was cooled in an acetone/dry-ice bath to -78 °C under a nitrogen atmosphere and treated with *n*-BuLi (170 μL, 2.5 M in hexane, 0.40 mmol) in one portion via a syringe, the lithiation was monitored by TLC and upon completion (by TLC) 4-nitrobenzoyl chloride (78 mg, 42 mmol) was added in one portion to the reaction mixture and was stirred for a further 30 min. The ice bath was then removed and the mixture was allowed to warm up to room temperature (22 °C) and stirred for 30 min. The solution was then evaporated under vacuum. Purification by column chromatography (SiO_2, 10:1 hexanes/EtOAc), followed by recrystallization in hexanes, yielded (3,3,4,4,5,5-hexafluoro-2-(2-methyl-5-phenylthiophen-3-yl)cyclopent-

1-enyl)(4-nitrophenyl)methanone (123 mg, 65%) as a yellow solid. Mp = 95-96 °C, (lit. 95-97 °C).[30]

^{1}H NMR ($CDCl_3$, 500 MHz): δ (ppm) = 8.19 (d, J = 9 Hz, 2H), 7.86 (d, J = 9 Hz, 2H), 7.36 (m, 5H), 7.11 (s, 1H), 2.27 (s, 3H).[30]

2-3,3,4,4,5,5-Hexafluoro-2-(2-methyl-5-phenylthiophen-3-yl)cyclopent-1-enyl)(4-nitrophenyl)methylene)malononitri1e (**1.24o**)

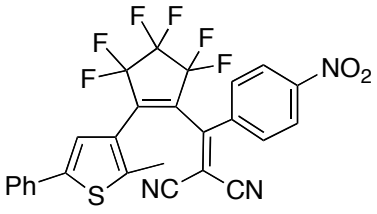

A solution of (3,3,4,4,5,5-Hexafluoro-2-(2-methyl-5-phenylthiophen-3-yl)cyclopent-1-enyl)(4-nitrophenyl)methanone (100 mg, 0.20 mmol) and malononitrile (33 mg, 0.50 mmol) in anhydrous dichloroethane (10 mL) was cooled in an ice bath to 0 °C under a nitrogen atmosphere and treated with $TiCl_4$ (0.19 mL, 0.9 mmol) drop-wise. After stirring for 5 min, pyridine (0.35 mL, 4.4 mmol) was added drop-wise over a period of 20 min. The ice bath was removed and the mixture was allowed to warm up to room temperature (22 °C). The red brown solution was heated at reflux for 10 min during which time a precipitate formed and the color changed to yellow-brown. After cooling back to room temperature (22 °C), the solvents were evaporated under reduced pressure. The solid green-brown residue was dissolved in HCl (20 mL, 1.8 M) with vigorous stirring, the aqueous layer was separated and extracted with chloroform (3 × 10 mL) and the combined organic layers were dried over Na_2SO_4, filtered and evaporated under

vacuum. Purification by column chromatography (SiO_2, 10:1 hexane/acetone) yielded 2-((3,3,4,4,5,5-hexafluoro-2-(2-methyl-5-phenylthiophen-3-yl)cyclopent-1-enyl)(4-nitrophenyl)methylene)malononitrile (65 mg, 60%) as an orange-red oil.

^{1}H NMR ($CDCl_3$, 500 MHz): δ (ppm) = 8.33 (d, J = 9 Hz, 2H), 7.67 (d, J = 9 Hz, 2H), 7.34 (m, 5H), 6.77 (s, 1H), 2.46 (s, 3H).[30]

Photochemical ring-closing of 2-{{3,3,4,4,5,5-Hexafluoro-2-{2-methyl-5-phenylthiophen-3-yl)cyclopent-1-enyl){4-nitrophenyl)methylene)malononitrile (**1.24c**)

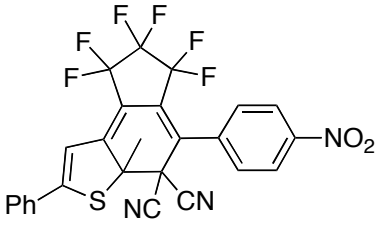

A standard glass NMR tube was charged with a 1 mL C_6D_6 solution containing 1 mg of **1.24o**. The entire tube was irradiated with 313 nm light from a handheld TLC visualization lamp for 5 min intervals and monitored by ^{1}H NMR spectroscopy. Monitoring the methyl signal of the thiophene ring assessed the progress of the photocyclization. At this concentration and wavelength, approximately 15 min was required to reach the photostationary state (55 %). The majority of the remaining material was assigned as the ring-open isomer.

^{1}H NMR (C_6D_6, 500 MHz): δ (ppm) = 7.68 (d, 2H, J = 8 Hz), 6.91 (m, 2H), 7.03 (m, 5H), 6.71 (s, 1H), 1.29 (s, 3H).[30]

2.4.6 Inhibition Reactions

2.4.6.1 Inhibition of Karstedt's catalyst by model compounds

2.4.6.1.1 Inhibition of Karstedt's catalyst as monitored by ^{1}H NMR spectroscopy

Stock solution preparation:

Karstedt's catalyst stock solution: Karstedt's catalyst in DVTMS (0.01 mL, 100 mM, 0.001 mmol) was diluted with C_6D_6 (0.09 mL).

*vinyltrimethylsilane(**2.7**)/triethylsilane(**2.8**) stock solution*: **2.7** (0.15 mL, 0.98 mmol) and **2.8** (0.08 mL, 0.50 mmol) were diluted with C_6D_6 (diluted to 1 mL).

Inhibition by 2.4

Karstedt's catalyst stock solution (0.10 mL, 1×10^{-4} mmol) was added to an NMR tube and diluted with C_6D_6 (0.20 mL) followed by the addition of inhibitor **2.5** (0. 7 mg, 3.5×10^{-3} mmol). The solution was heated to 50 °C for 1 h and then cooled for 20 min, the **2.8**/**2.7** stock solution was then added (0.10 mL, 0.010 mmol **2.7**, 0.005 mmol **2.8**). After letting stand for 45 min ^{1}H NMR spectra were taken.

Inhibition by 2.5

Karstedt's catalyst stock solution (0.10 mL, 1×10^{-4} mmol) was added to an NMR tube and diluted with C_6D_6 (0.20 mL) followed by the addition of **2.5** (0.05 mg, 3.2×10^{-3} mmol). The solution was heated to 50 °C for 1 h and then cooled for 20 min, the **2.8**/**2.7** stock solution was then added (0.10 mL, 0.010 mmol **2.7**, 0.005 mmol **2.8**). After letting stand for 45 min ^{1}H NMR spectra were taken.

Inhibition by 2.6

Karstedt's catalyst stock solution (0.10 mL, 1×10^{-4} mmol) was added to an NMR tube and diluted with C_6D_6 (0.20 mL) followed by the addition of **2.6** (0.07 mg, 3.8×10^{-3} mmol). The solution was heated to 50 °C for 1 h and then cooled for 20 min, the **2.8**/**2.7** stock solution was then added (0.10 mL, 0.010 mmol **2.7**, 0.005 mmol **2.8**). After letting stand for 45 min ^{1}H NMR spectra were taken.

Inhibition by 2.3

Karstedt's catalyst stock solution (0.10 mL, 1×10^{-4} mmol) was added to an NMR tube and diluted with C_6D_6 (0.20 mL) followed by the addition of **2.3** (0.05 mg, 3.5×10^{-3} mmol). The solution was heated to 50 °C for 1 h and then cooled for 20 min, the **2.8**/**2.7** stock solution was then added (0.10 mL, 0.010 mmol **2.7**, 0.005 mmol **2.8**). After letting stand for 45 min ^{1}H NMR spectra were taken.

Control reaction (no inhibitor)

Karstedt's catalyst stock solution (0.10 mL, 1×10^{-4} mmol) was added to an NMR tube and diluted with C_6D_6 (0.20 mL). The solution was heated to 50 °C for 1 h and then cooled for 20 min, the **2.8**/**2.7** stock solution was then added (0.10 mL, 0.010 mmol **2.7**, 0.005 mmol **2.8**). After letting stand for 45 min ^{1}H NMR spectra were taken.

2.4.6.1.2 Inhibition of Karstedt's catalyst as monitored by gas chromatography

Stock solution preparation:

*vinyltrimethylsilane(**2.7**)/triethylsilane(**2.8**)/decane* stock solution: **2.8** (0.16 mL, 1.0 mmol), **2.7** (0.32 mL, 1.9 mmol) and decane (0.04 mL, 0.21 mmol)

***2.4** stock solution*: **2.4** (14 mg, 0.073 mmol) was dissolved with toluene (4 mL).

2.5 *stock solution*: **2.5** (11 mg, 0.073 mmol) was dissolved with toluene (4 mL).

Inhibition by 2.4

To a portion of **2.4** stock solution (1 mL, 0.018 mmol), the catalyst in xylenes (6 μL, 0.0005 mmol) was added and the solution was incubated at 50 °C for 1 h. To this, **2.8**/**2.7** stock solution (130 μL, 0.25 mmol of **2.8**, 0.49 mmol of **2.7**) was added and the reaction was held at 30 °C by a water bath and monitored by GC.

Inhibition by 2.5

To a portion of 2.5 stock solution (1 mL, 0.018 mmol) catalyst in xylenes (6 μL, 0.0005 mmol) was added and the solution was incubated at 50 °C for 1 h. To this, **2.8**/**2.7** stock solution (130 μL, 0.25 mmol of **2.8**, 0.49 mmol of **2.7**) was added and the reaction was held at 30 °C by a water bath and monitored by GC.

Control (no inhibitor)

Catalyst in xylenes (6 μL, 0.0005 mmol) was added to toluene (1 mL) and the solution was incubated at 50 °C for 1 h. To this, **2.8**/**2.7** solution (130 μL, 0.25 mmol of **2.8**, 0.49 mmol of **2.7**) was added and the reactions were held at 30 °C by a water bath and monitored by GC.

2.4.6.2 Inhibition of Karstedt's catalyst by DCTE

2.4.6.2.1 Inhibition of Karstedt's catalyst as monitored by ^{1}H NMR spectroscopy

Stock solution preparation:

1.24o *stock solution*: **1.24o** (5 mg, 0.009 mmol) was diluted with C_6D_6 (1.5 mL).

Karstedt's catalyst stock solution: Karstedt catalyst solution (0.10 mL, 100 mM, 0.01 mmol) was diluted with C_6D_6 (diluted to 1 mL) this solution was furthered diluted with C_6D_6 (10 ×, 0.1 mL in 1 mL).

*Triethylsilane(**2.8**)/vinyltrimethylsilane(**2.7**) stock solution:* vinyltrimethylsilane (0.40 mL, 2.6 mmol) and triethylsilane (0.20 mL, 1.3 mmol) were diluted with C_6D_6 (0.3 mL), a portion (0.3 mL) of this solution is then diluted with C_6D_6 (0.7 mL).

Inhibition by 1.24o (solution that was not irradiated)

To a 1 dram vial, **1.24o** stock solution (0.50 mL, 0.003 mmol) was added. The vial was then charged with catalyst stock solution (0.10 mL, 0.0001 mmol), and incubated at 50 °C for 1 h with a hot water bath and then cooled to room temperature. At this point **2.7**/**2.8** stock solution (0.10 mL, 0.043 mmol **2.8**, 0.087 mmol **2.7**) was added, this time was considered to be t_0. Successive ^{1}H NMR spectra were taken for 1 h.

Inhibition by 1.24o/1.24c (solution that was irradiated).

To a 1 dram vial, **1.24o** stock solution (0.50 mL, 0.003 mmol). The vial was then charged with catalyst stock solution (0.10 mL, 0.0001 mmol), and incubated at 50 °C for 1 h with a hot water bath and then cooled to room temperature. At this point **2.7**/**2.8** stock solution (0.10 mL, 0.043 mmol **2.8**, 0.087 mmol **2.7**) was added, this time was considered to be t_0. Successive ^{1}H NMR spectra were taken for this solution for 30 min, at which point the solution was irradiated with 313 nm light for 9 min. ^{1}H NMR spectra were then taken for a further 30 min.

Control Reaction (no inhibitor)

To a 1 dram vial, C_6D_6 (0.05 mL) was added. The vial was then charged with catalyst stock solution (0.10 mL, 0.0001 mmol), and incubated at 50 °C for 1 h with a hot water bath and then cooled to room temperature. At this point **2.7**/**2.8** stock solution (0.10 mL, 0.043 mmol **2.8**, 0.087 mmol **2.7**) was added, this time was considered to be t_0. Successive ^{1}H NMR spectra were taken for solution for 30 min, at which point the solution was irradiated with 313 nm light for 9 min. ^{1}H NMR spectra were then taken for a further 30 min.

2.4.6.2.2 Inhibition of Karstedt's catalyst as monitored by gas chromatography

Stock solution preparation:

*Vinyltrimethylsilane(**2.7**)/triethylsilane(**2.8**)/decane stock solution*: triethylsilane (0.14 mL, 0.88 mmol), vinyltrimethylsilane (0.28 mL, 1.7 mmol) and decane (0.04 mL, 0.21 mmol).

***1.24o** stock solution*: **1.24o** (20 mg, 0.037 mmol) was dissolved in C_7H_8 (8 mL).

Inhibition by 1.24o

To a portion of **1.24o** stock solution (4 mL, 0.019 mmol) catalyst in xylenes (6 μL, 0.0005 mmol) was added and the solutions were incubated at 50°C for 1 h. To this, **2.8**/**2.7** stock solution (116 μL, 0.22 mmol of **2.8**, 0.44 mmol of **2.7**) was added and the reaction was held at 30 °C by a water bath and monitored by GC.

Inhibition by 1.24c

To a portion of **1.24o** stock solution (4 mL, 0.019 mmol) was irradiated with 313 nm light for 15 min, after which it was concentrated down to 1 mL. To this, catalyst in xylenes (6 μL, 0.0005 mmol) was added and the solutions were incubated at 50° C for

1 h. To this, **2.8**/**2.7** stock solution (116 μL, 0.22 mmol of **2.8**, 0.44 mmol of **2.7**) was added and the reaction was held at 30 °C by a water bath and monitored by GC.

Control

Catalyst in xylenes (6 μL, 0.0005 mmol) was added to toluene (1 mL) and the solution was incubated at 50 °C for 1 h. To this, **2.8**/**2.7** s solution (116 μL, 0.22 mmol of **2.8**, 0.44 mmol of **2.7**) was added and the reactions were held at 30 °C by a water bath and monitored by GC.

3 DETERMINING THE INTERACTION BETWEEN INHIBITORS AND KARSTEDT'S CATALYST BY NMR SPECTROSCOPY

3.1 General introduction to the determination of binding affinities

One way to measure the interaction between two complexes is to measure the binding affinity. In a typical system there exists two species often referred to as a host, **A** (Karstedt's catalyst) and a guest, **B** (inhibitor); together they form a complex, **C**. For this type of interaction, *Equation* 3.1 describes the equilibrium.

$$a\mathrm{A} + b\mathrm{B} \rightleftharpoons c\mathrm{C}$$

Equation 3.1 Complex (**C**) formation between a host (**A**) and a guest (**B**).

The binding constant **K**, or the equilibrium constant, is a stability constant for the formation of the complex, and is determined by the concentration of the guest [B], the host [A] and the complex [C] at equilibrium (*Equation* 3.2). Consequently, it is necessary to determine the concentration of each species to evaluate the binding constant of the host-guest complex.[34]

$$\mathrm{K} = \frac{[\mathrm{C}]^c}{[\mathrm{A}]^a \cdot [\mathrm{B}]^b}$$

Equation 3.2 Equilibrium constant (**K**) determination from the concentration of host [**A**], guest [**B**] and complex [**C**].

Nuclear magnetic resonance (NMR) spectroscopy is an effective technique to determine the concentration of species in solution and is widely used for the evaluation of binding constants.[35] Generally, nuclei involved in complex formation are partitioned between two non-equivalent environments, and therefore have different chemical shifts

from their bound forms. The nature of the NMR signal depends on the complexation rate (k) and decomplexation rate (k').

$$a\mathrm{A} + b\mathrm{B} \underset{\mathrm{k'}}{\overset{\mathrm{k}}{\rightleftharpoons}} c\mathrm{C}$$

Equation 3.3 Rates of reaction for complex formation, k and k'.

3.2 Fast and slow exchanges

Depending on the rate of exchange, relative to the NMR timescale, the nature of the signal can vary, as illustrated in *Figure 3.1*. For slow exchanges, the two species are present long enough that their bound and unbound states can be seen individually. For fast exchanges, the complexation and decomplexation rates are too fast to obtain separate signals and instead a single signal is observed which corresponds to the weighted average of both species.

In both fast and slow exchanges, it is possible to determine binding constants (K) by performing titrations and plotting titration curves of equivalents of host added (catalyst in this case) versus change in chemical shift, or appearance of new signals.

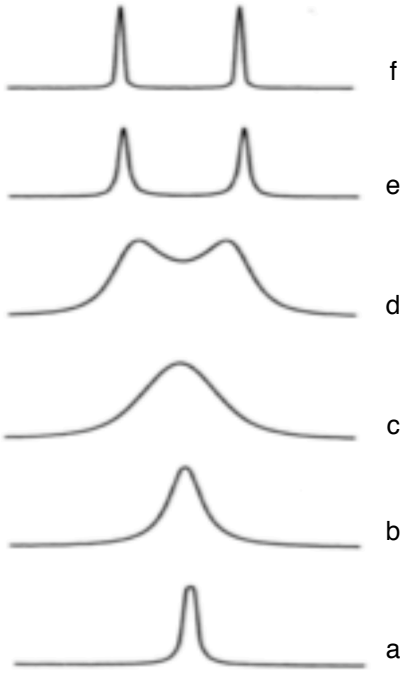

Figure 3.1 NMR signals of a hypothetical guest host complex: a) slow exchange limit; b) c) moderately slow exchange; d) coalescence; e) moderately fast exchange; f) fast exchange.

3.2.1 Determining binding affinities for Karstedt's catalyst

In order to calculate binding affinities for any two molecules the concentration of each molecule must be known, however, this is not possible for Karstedt's catalyst. As discussed in *Section 1.1.3*, Karstedt's catalyst can exist in several forms, and the inhibited complex also likely exists in several forms, making the determination of their concentrations not possible. The complexity of Karstedt's catalyst has also made kinetic studies of the catalyst problematic; and currently, there is no established rate law for Karstedt-catalyzed hydrosilylation reactions, as the rate law has been shown to depend on the relative concentration of the reactants involved. For example, if the vinyl silane is the limiting reagent then the catalysis proceeds through an entirely different mechanism[9]; furthermore, the type of ligand bound to the catalyst can also affect the rate law.[36]

Consequently it will not be possible to determine binding affinities for Karstedt's catalyst complexes, however it will be possible to assess whether the inhibitor is interacting with the catalyst in a qualitative manner.

3.3 NMR spectroscopy as a screening tool for inhibitors

Presumably, if a molecule inhibits Karstedt's catalyst the inhibited complex will have a different ^{1}H NMR signal that the non coordinated species. Molecules that do not inhibit Karstedt's catalyst and therefore do not interact with the catalyst will show no changes in their ^{1}H NMR spectra upon addition to the catalyst. As a result, ^{1}H NMR spectroscopy could serve as a screening tool for inhibitors, seeing as it is much faster than carrying out actual hydrosilylation reactions; if a molecule is shown to interact with the catalyst by NMR spectroscopy, then further analysis by hydrosilylation reactions could be pursued.

3.4 New molecules to be tested as Karstedt catalyst inhibitors

Recording a NMR spectrum is much faster than performing hydrosilylation reactions, and a greater number of candidate inhibitors can be screened. In addition to the molecules already tested in *Chapter 2*, a variety of other molecules were tested as described below.

3.4.1 A sterically unhindered DCTE

One molecule possessing the characteristics needed to inhibit Karstedt's catalyst is shown in *Figure 3.2*. The molecule contains the necessary electron deficient alkene but is not sterically hindered like **1.24o** as it does not contain a phenyl ring. Unfortunately, **1.25o** can not be used practically as it has a very low photostationary state (18%)[30];

however, if **1.25o** can bind to the catalyst then this would support the hypothesis that **1.24o** was unable to inhibit because it is sterically hindered.

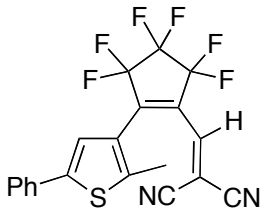

1.25o

Figure 3.2 DCTE **1.25o** contains an unhindered electron deficient double bond

3.4.2 Dithienylethenes (DTE) containing electron deficient alkenes that are not part of the hexatriene

One alternative is to have a photoswitch in which the closed-form inhibits the catalysis; therefore, the photostationary state is not an issue as long as the open-form does not also inhibit. In this type of system the closed-form (or a solution of the photostationary state) would be added to the catalyst where the closed-form present will inhibit the catalyst and any open-form present will have no effect. In this type of system the electron deficient alkene would not be part of the hexatriene system; instead, the molecule would possess an electron deficient alkene which is more electron deficient in the closed-form. These types of systems exist with dithienylethenes. Examples of which are shown below (*Figure 3.3*). In these molecules, upon ring closure, the two π systems become conjugated and in effect become more electron deficient. For these molecules, as there is no precedent for inhibition using these molecules, it was necessary to determine if either form inhibits catalysis before performing titration experiments with the catalyst. Furthermore, both of these molecules have photostationary states greater than 95%.

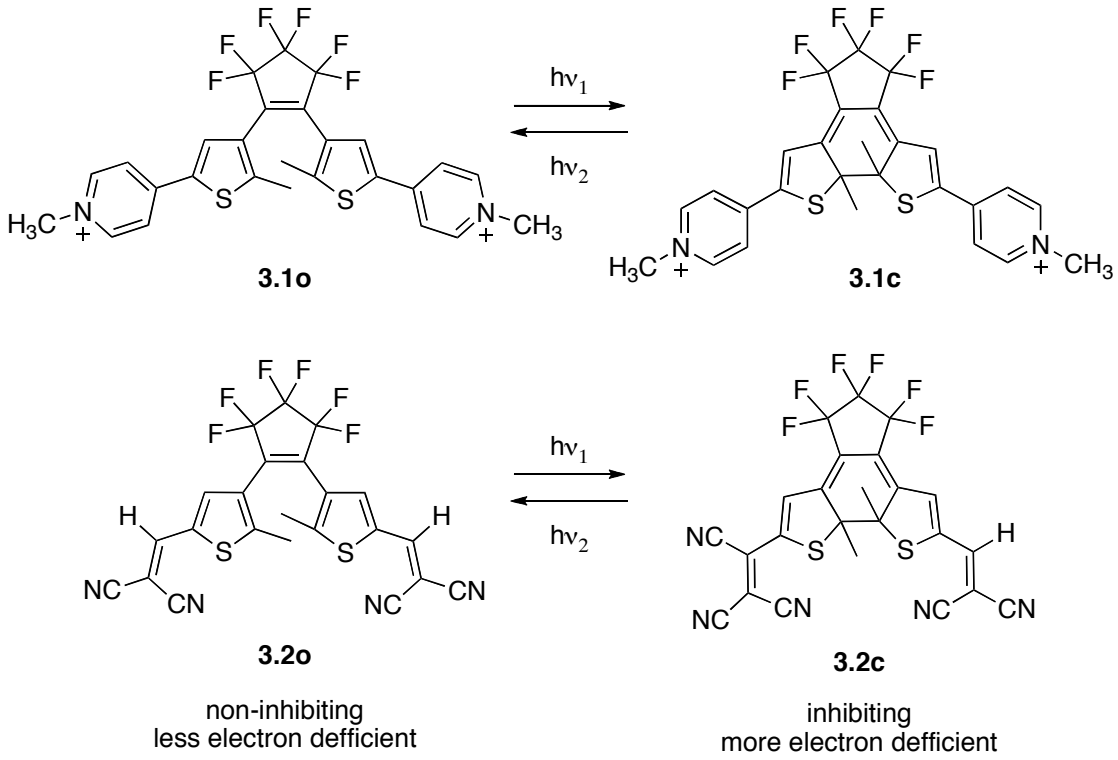

Figure 3.3 New DTE molecules to be tested, **3.1o** and **3.2o,** in which the closed-form would be inhibiting and the open-form would be uninhibiting.

3.5 Results and Discussion

3.5.1 Synthesis

3.5.1.1 Synthesis of DCTE 1.25o

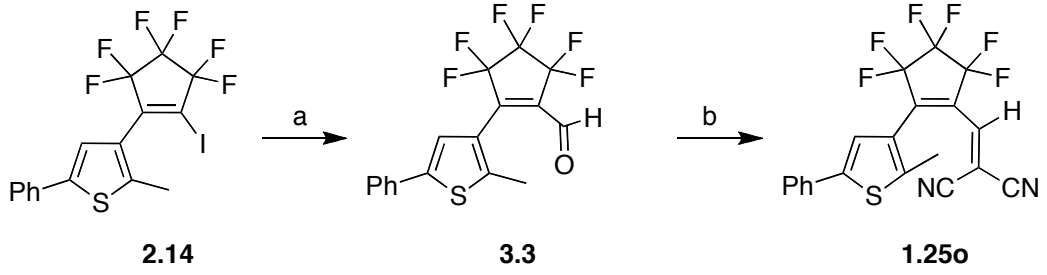

Scheme 3.1 Synthesis of **1.25o** from the previously synthesized precursor **2.14**. Reaction conditions: a) 1. *n*-BuLi, 2. DMF, Et_2O, -78 °C, 15%; b) $CH_2(CN)_2$, $TiCl_4$, pyridine, DCE, reflux, 35%.

1.25o was synthesized according to the previously reported synthesis, as shown in *Scheme* 3.1.[30] Starting from **2.14**, which is treated with *n*-BuLi and quenched with DMF generating **3.3** in 15% yield as indicated by the presence of the aldehyde proton in the ^{1}H NMR spectrum. This low yield is attributed to the highly reactive lithiated intermediate which can react with itself as well as the un-lithiated starting material. A Knoevenagel condensation afforded **1.25o** in 35% yield which is indicated by the shifting upfield of the dicyanoethylene proton in the ^{1}H NMR spectrum.[30]

3.5.1.2 Synthesis of DTE

The pyridinium salt **3.1o** was generously provided by Dr. Jeremy Finden,[37] and **3.2o** was synthesized with modification from a previously reported synthesis[38] as shown in *Scheme 3.2*. The chlorothiophene (**3.5**), a common building block for symmetric DTE's, is treated with *t*-BuLi, followed by DMF affording **3.6** in 34% yield. Treatment with malononitrile yields **3.2o** in 60% yield..

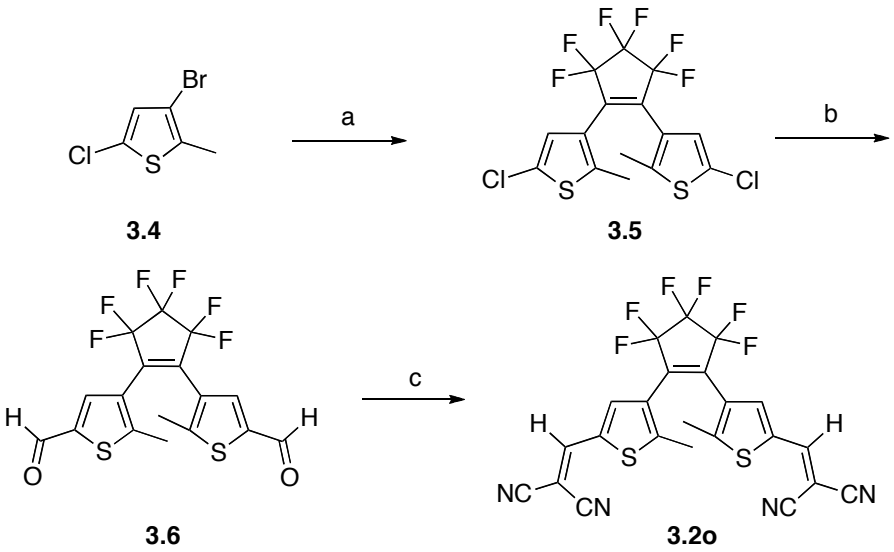

Scheme 3.2 Synthetic scheme for **3.2o**. Reaction conditions: a) 1. *n*-BuLi, 2. C_5F_8, Et_2O, -78 °C, 45%; b) 1. *t*-BuLi, 2. DMF, Et_2O, -78 °C, 34%; c) $CH_2(CN)_2$, piperidine, EtOH, reflux, 60%.

3.5.2 Binding studies between Karstedt's catalyst and proposed inhibitors

3.5.2.1 Binding of Karstedt's catalyst and 1.24o

The interaction between **1.24o** and Karstedt's catalyst was evaluated by titration of **1.24o** with Karstedt's catalyst as shown in *Figure 3.4*, for clarity only the proton resonance assigned to the thiophene proton is plotted.

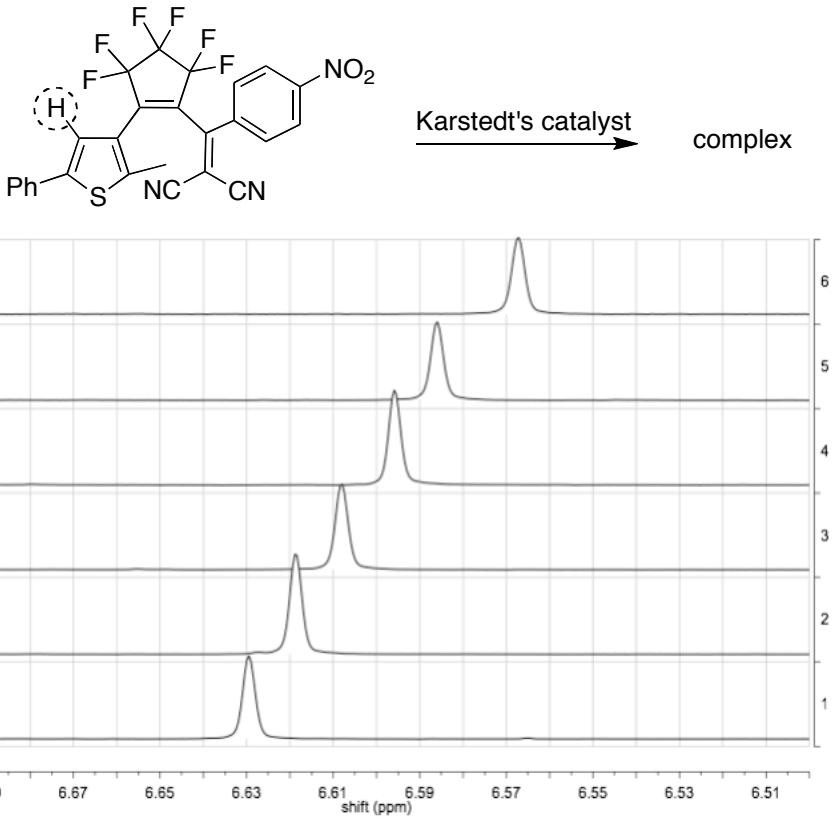

Figure 3.4 Change in the thiophene proton resonance in the ^{1}H NMR spectrum of **1.24o** as Karstedt's catalyst is added in successive equivalents. Spectrum 1:**1.24o** before addition of catalyst**,** 2: 0.2 eq., 3: 0.4 eq., 4: 0.7 eq., 5: 1 eq, 6: 2 eq.

As *Figure 3.4* above shows there is a noticeable shift in the ^{1}H NMR signals of **1.24o** as Karstedt's catalyst is added, suggesting there is an interaction between the catalyst and the **1.24o**. This interaction is fast as compared to the NMR spectroscopy

timescale (milliseconds). The above data can also be plotted on a graph showing the change in signal as a function of equivalents of **1.24o** added (*Figure 3.5*).

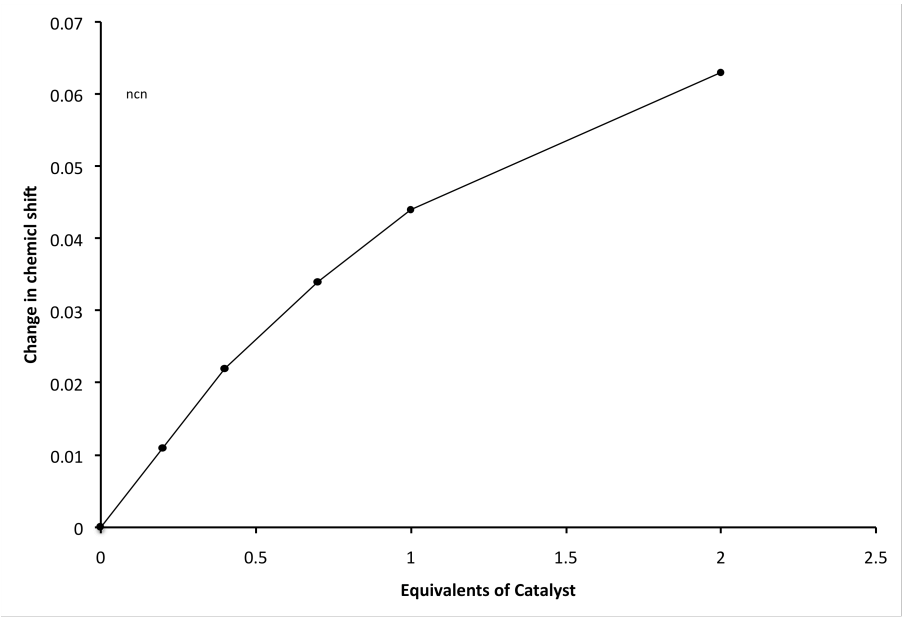

Figure 3.5 Change in ^{1}H NMR chemical shift (δ) for **1.24o** as a function of catalyst equivalents added.

3.5.2.2 Binding study for Karstedt's catalyst and 2.4

The same titration experiment was conducted for **2.4**, which was known to inhibit the catalyst. However, a change in signal was not observed (*Figure 3.6*). Instead an additional set of signals were observed as the catalyst was added, with a corresponding decrease in the integration of **2.4**. These new signals were attributed to the bound complex, suggesting a slower exchange rate. This data was also plotted on a graph as a ratio of bound **2.4** to unbound **2.4** as a function of equivalents of Karstedt's catalyst (*Figure 3.7*). For clarity only one of the phenyl doublets is plotted.

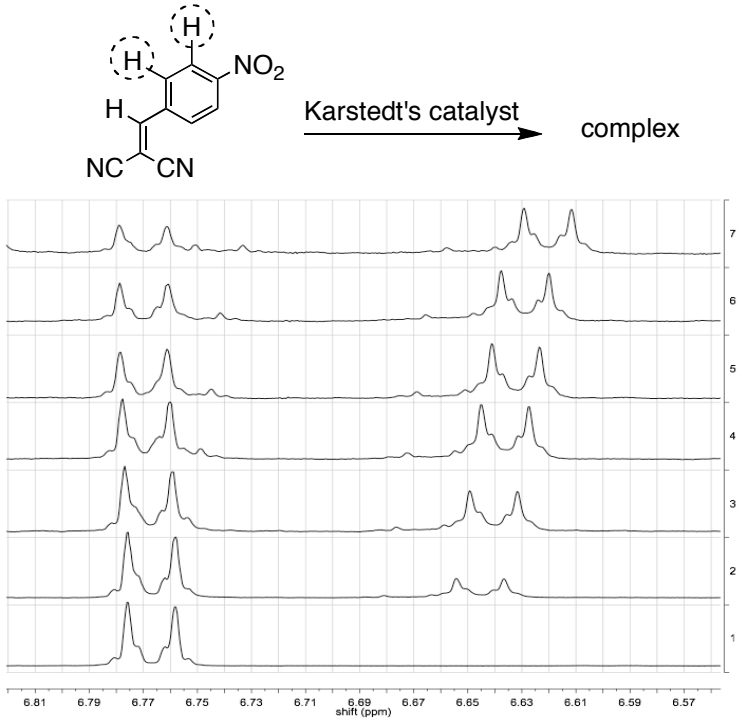

Figure 3.6 Change in the ^{1}H NMR spectrum corresponding to the phenyl region of **2.4** as successive equivalents of Karstedt catalyst are added**.** Spectrum 1: **2.4** before the addition of catalyst**.** 2: 0.3 eq., 3: 0.6 eq., 4: 0.9 eq., 5: 1.2 eq. 7, 6: 1.8 eq., 7: 3 eq.

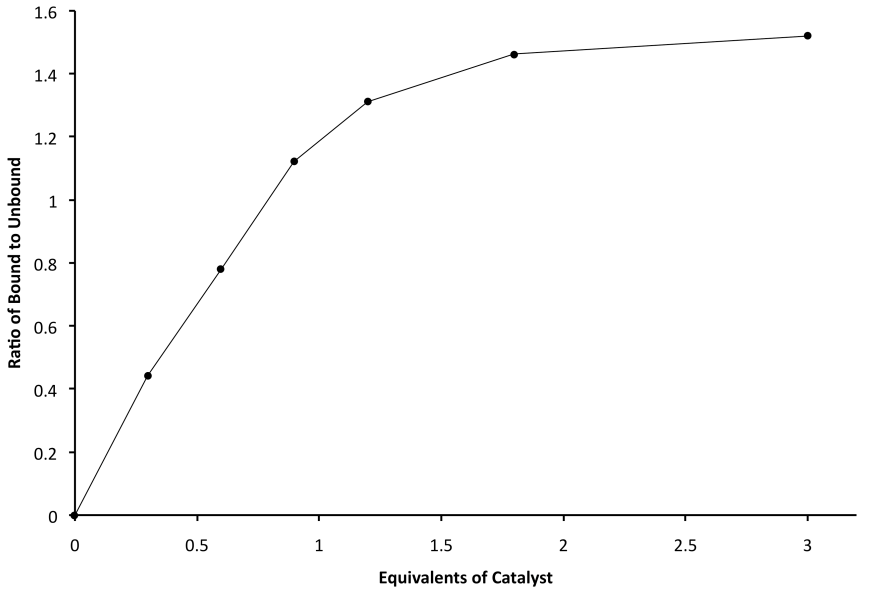

Figure 3.7 Ratio of bound **2.4** to unbound **2.4** as a function of catalyst equivalents added.

3.5.2.3 Binding study for Karstedt's catalyst and 1.25o

A ^{1}H NMR titration study was performed for **1.25o**, in the same fashion as those performed for **1.24o** and **2.4.** The results are shown in *Figure 3.8* and *Figure 3.9*. For clarity only one of the phenyl proton signals is plotted.

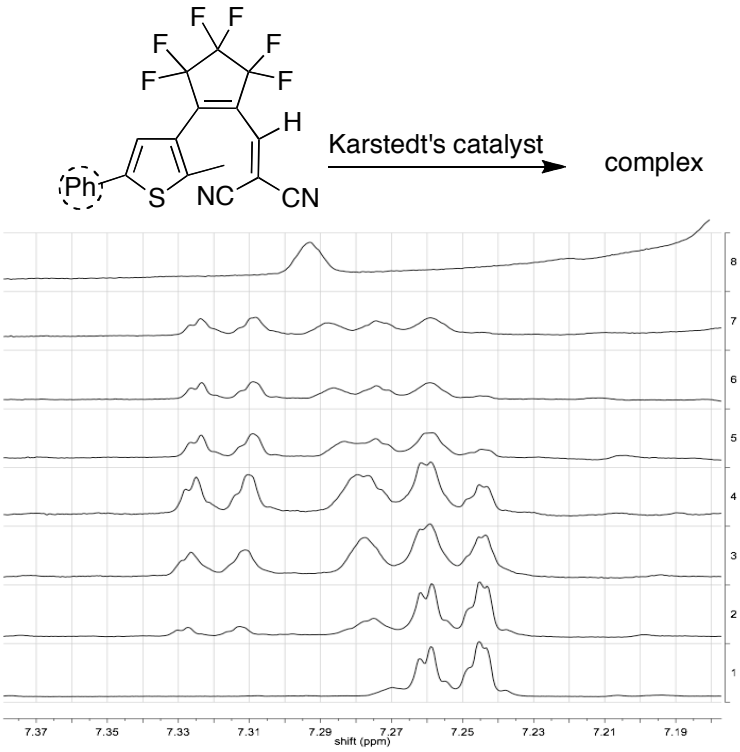

Figure 3.8 Change in the ^{1}H NMR spectrum corresponding to the phenyl region of **1.25o** as successive equivalents of 0.15, 0.30, 0.6, 1.2, 1.8, 3. Spectrum 8 is a background reference spectrum for Karstedt's catalyst and spectrum 1: **1.25o** before the addition of catalyst 2: 0.15 eq., 3: 0.3 eq., 4: 0.6 eq., 5: 1.2 eq., 6: 1.8 eq., 7: 3 eq., 8: Karstedt's catalyst (background). Phenyl protons are shown.

Similar to **2.4**, a change in signal was not observed in the ^{1}H NMR spectrum (*Figure 3.8*). Instead an additional set of signals was observed as the catalyst was added, with a corresponding decrease in the integration of the phenyl protons of **1.25**, which also indicates that a complex with a slow exchange is forming between the two species. As with the other molecules a titration curve was graphed; however, it should be noted that

the unbound signal of **1.25o** is overlapping with the unbound catalyst signals and therefore the values obtained are only approximations. The phenyl proton signal was the only signal in the spectrum that could be used because other signals were directly overlapping with Karstedt catalyst signals.

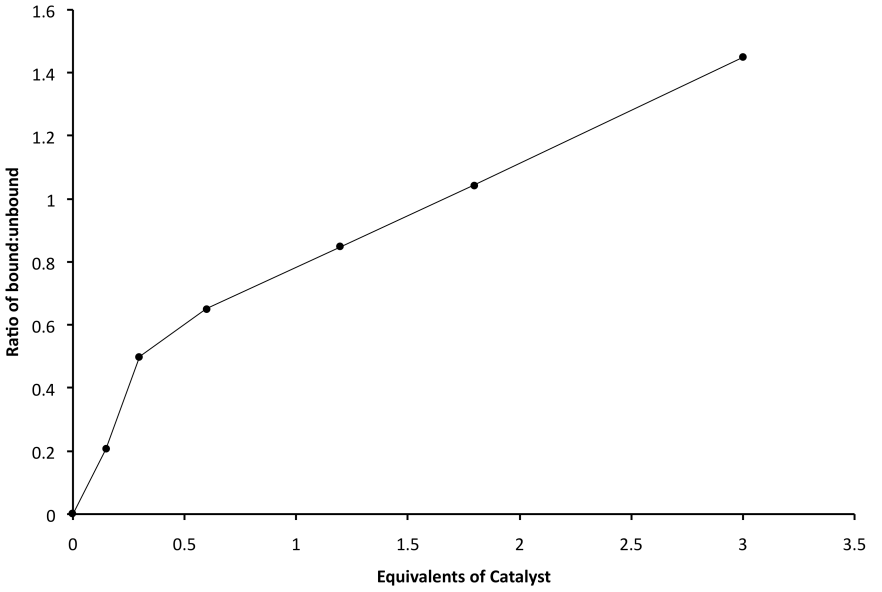

Figure 3.9 Ratio of bound **1.25o** to unbound **1.25o** as a function of catalyst equivalents added.

Although these results provided good insight into the nature of the interaction between the DCTE's and the catalyst, **1.25o** could not be used as it had a low photostationary state (18%). Practically speaking even though **1.25o** is a good inhibitor, its irradiation would only result in a slight decrease in it's concentration. An attempt at increasing the photostationary state by scanning different wavelengths was unsuccessful.

3.5.2.4 Binding study for Karstedt's catalyst with 3.1o and 3.1c

To test for binding and therefore inhibition, Karstedt's catalyst was added to a solution of **3.1o**, along with a solution of the photostationary state (*i.e.* a solution containing open and closed-forms of the molecule).

The titration experiment for **3.1o** and **3.1c** is shown in *Figure 3.10*; spectrum 1 shows **3.1o** and spectrum 2 shows **3.1o** added to Karstedt's catalyst. There is no shift in signals and no new signals. The same is true for the closed form. Spectrum 3 shows **3.1c** and spectrum 4 shows **3.1c** added to Karstedt's catalyst - no shift in signal is observed nor any new signals. These observations indicate no interaction of **3.1o/c** with Karstedt's catalyst and as a result, the molecule should not be used as an inhibitor.

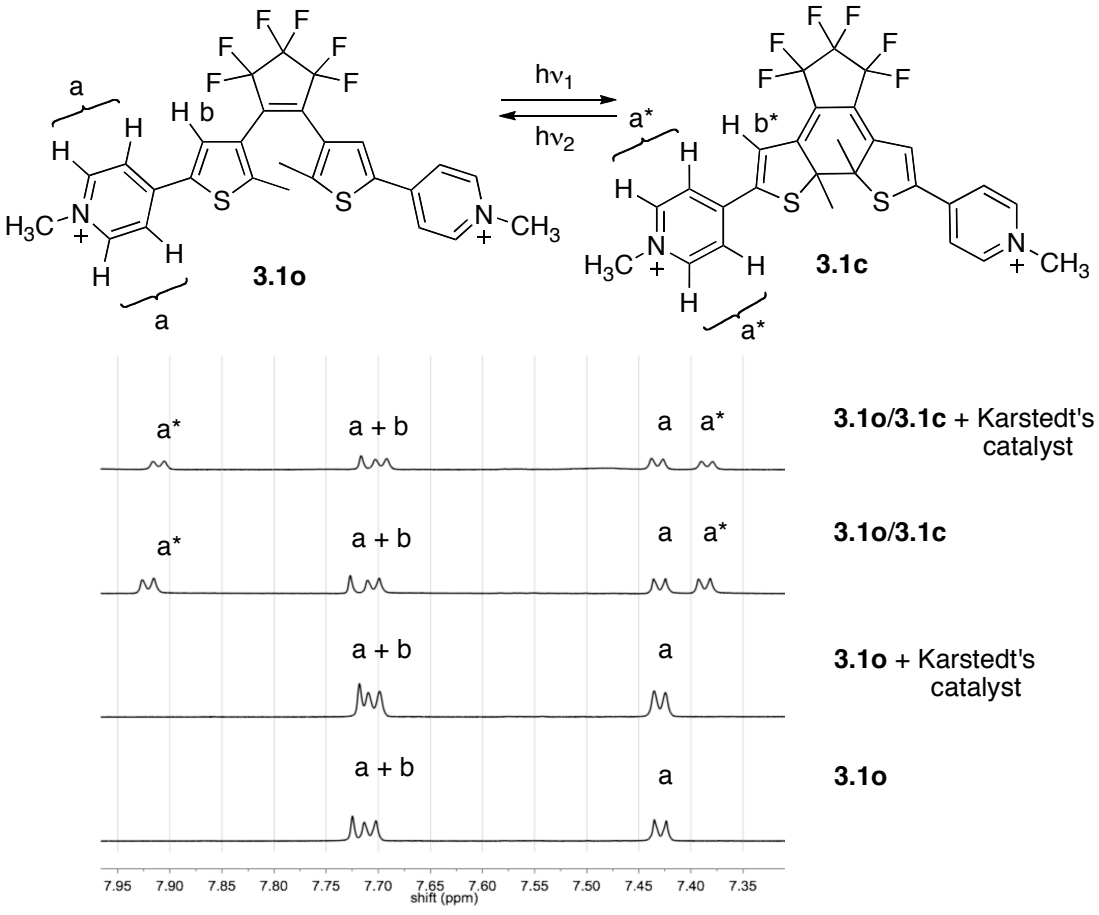

Figure 3.10 ^{1}H NMR spectrum of **3.1o** and **3.1c** before and after the addition of Karstedt's catalyst. Spectrum 1: **3.1o**; spectrum 2: **3.1o** + Karstedt's catalyst; spectrum 3: **3.1o/3.1c**; spectrum 4: **3.1o/3.1c** + Karstedt's catalyst

3.5.2.5 Binding study for Karstedt's catalyst with 3.2o and 3.2c

The titration experiment for **3.2o** and **3.2c** is shown in *Figure 3.11*. Spectrum 1 shows **3.2o** and spectrum 2 shows **3.2o** added to Karstedt's catalyst. There is no shift in signals and no new signals. Spectrum 3 shows **3.2c** and spectrum 4 shows **3.2c** added to Karstedt's catalyst. Interestingly, when the catalyst was added to **3.2c** the molecule ring opened. Further investigation into this phenomenon may be warranted, but is beyond the scope of this project. Ultimately, neither molecule showed any coordination to Karstedt's catalyst.

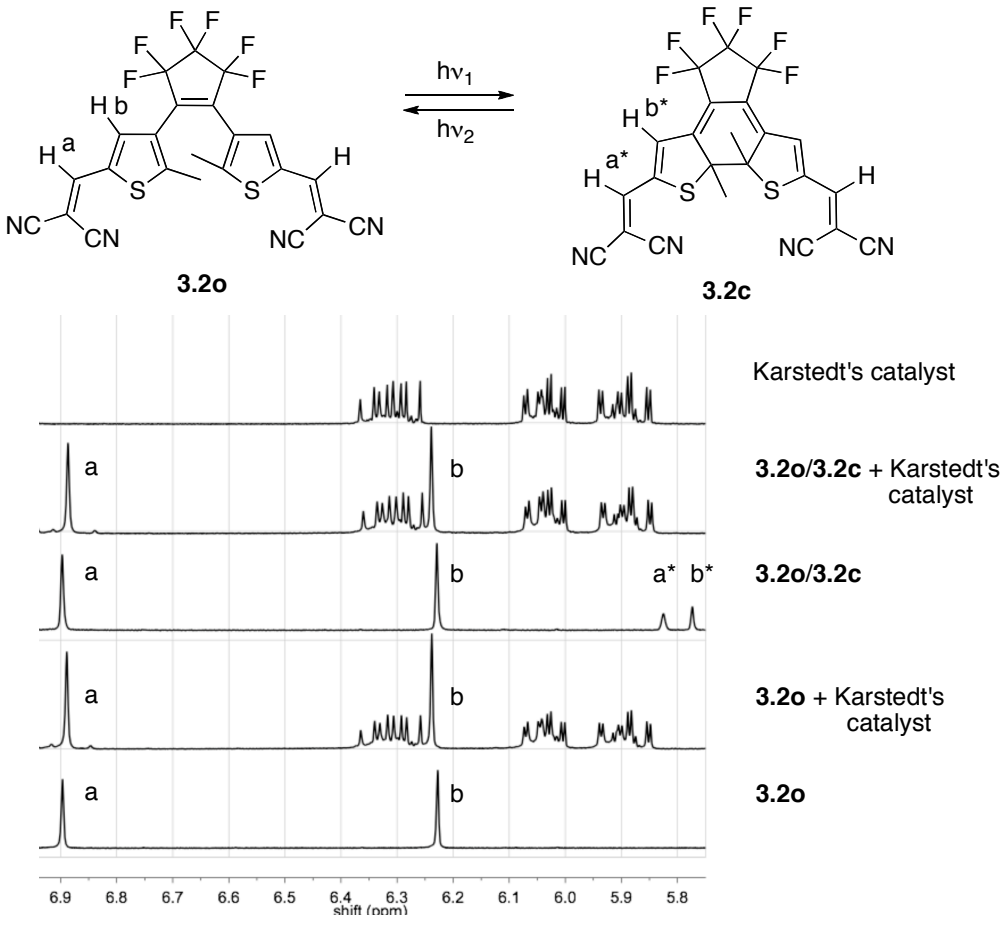

Figure 3.11 ^{1}H NMR spectrum of **3.2o** and **3.2c** before and after the addition of with Karstedt's catalyst. Spectrum 1: **3.2o**; spectrum 2: **3.2o** + Karstedt's catalyst; spectrum 3: **3.2o**/**3.3c**; spectrum 4: **3.2o**/**3.2**c + Karstedt's catalyst; spectrum 5: Karstedt's catalyst.

3.6 Conclusion

In conclusion, the data presented in this chapter provided greater insight into the binding of inhibitors to Karstedt's catalyst. From the data it is reasonable to assume that **1.24o** did not inhibit the catalyst because of the steric bulk around the coordination site of the DCTE. Unfortunately, it was not possible to calculate binding constants for the Karstedt-inhibitor complexes due to the complexity of the catalyst. However, the data suggests that slow exchanges as indicated by NMR spectroscopy may provide for better inhibition of Karstedt's catalyst, but further investigations are needed to confirm this hypothesis. For a molecule to inhibit Karstedt's catalyst their must be some interaction between the two, and although this interaction cannot be quantified, it can still be detected by NMR spectroscopy; consequently, in future experiments, NMR spectroscopy should be used as method to screen for Karstedt catalyst inhibitors.

3.7 Experimental

3.7.1 Materials

All solvents for metal-halogen exchange reactions were dried by refluxing over sodium. All other solvents were used as received. Solvents for NMR analysis (Cambridge Isotope Laboratories) were used as received. Column chromatography was performed using silica gel 60 (230-400 mesh) from Silicycle Inc., or with a Teledyne Isco CombiFlash Companion sg100c and redisep normal phase silica columns. All other reagents and starting materials including Karstedt's catalyst were purchased from Aldrich.

3.7.2 Techniques

^{1}H NMR characterizations were performed on a Varian Inova 600 instrument working at 599.8 MHz for 1H NMR. Chemical shifts (δ) are reported in parts per million relative to tetramethylsilane using the residual solvent signal as a reference standard: $CDCl_3$ (δ = 7.26 ppm), C_6D_6 (δ = 7.16 ppm). Coupling constants (J) are reported in Hertz. UV-VIS measurements were performed using a Varian Cary 300 Bio spectrophotometer. Melting point measurements were performed using a Fisher-Johns melting point apparatus.

3.7.2.1 Photochemistry

Standard lamps used for visualizing TLC plates (Spectroline E-series, 470 *mW/cm^2)* were used to carry out all the ring closed reactions. A 313 nm light source was used.

3.7.3 Synthetic Methods

3,3,4,4,5,5-Hexafluoro-2-(2-methyl-5-phenylthiophen-3-yl)cyclopent-1-enecarbaldehyde (**3.3**)

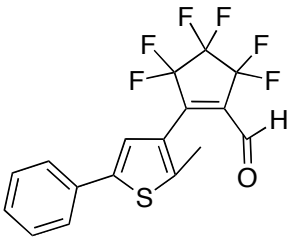

A solution of 3-(3,3,4,4,5,5-Hexafluoro-2-iodocyclopent-1-enyl)-2-methyl-5-phenylthiophene (**2.14**), (100 mg, 0.21 mmol) in anhydrous Et_2O (5 mL) was cooled in an acetone/dry-ice bath to -78 °C under a nitrogen atmosphere and treated with *n*-BuLi (90 μL, 2.5 M in hexane, 0.23 mmol) in one portion via a syringe. The resulting pale yellow solution was stirred for an additional 15 min at – 78 °C, upon which anhydrous DMF (65 μL, 0.84 mmol) was added in one portion to the reaction mixture using a syringe. The resulting blue-black mixture was stirred for another 15 min at – 78 °C, and then allowed to warm to room temperature (22 °C). After quenching with saturated aqueous NH_4CI (50 mL) the aqueous layer was separated and extracted with Et_2O (3 × 5 mL). The combined organic layers were washed with water, then brine, dried over Na_2SO_4, filtered and evaporated to dryness under vacuume. Purification by column chromatography (SiO_2, hexanes/EtOAc 6:1), and further purification using a Chromatatron™, centrifugal thin-layer chromatograph, (1mm plate, SiO_2, hexanes/EtOAc 10:1). Further purification by recrystallization in hexanes yielded 23 mg of 3,3,4,4,5,5-hexafluoro-2-(2-methyl-5-phenylthiophen-3-yl)cyclopent-1-enecarbaldehyde (30%) as a yellow solid. Mp = 89-90 °C (lit. 80-90 °C).[30]

^{1}H NMR ($CDCl_3$, 600 MHz): δ (ppm) = 2.48 (s, 3H), 7.35 (s, 1H), 7.38 (m, 1H), 7.42 (m, 2H), 7.56 (d, 2H, J = 8 Hz), 9.78 (s, 1H).[30]

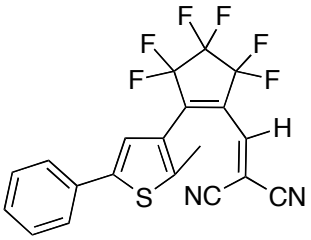

2-((3,3,4,4,5,5-Hexafluoro-2-(2-methyl-5-phenylthiophen-3-yl)cyclopent-1-enyl)methylene)malononitrile (**1.25o**)

A solution of 3,3,4,4,5,5-hexafluoro-2-(2-methyl-5-phenylthiophen-3-yl)cyclopent-1-enecarbaldehyde (40 mg, 0.11 mmol) and malononitrile (55 mg, 0.22 mmol) in anhydrous dichloroethane (5 mL) were cooled in an ice bath to 0 °C under a nitrogen atmosphere. The solution was then treated with $TiCl_4$ (0.1 mL, 0.9 mmol) drop-wise and stirred for 5 min, after which pyridine (0.2 mL, 2.5 mmol) was added drop-wise over 20 min. The ice bath was removed and the mixture was allowed to warm room temperature (22 °C) . The solution was heated at reflux for 10 min during which time a precipitate formed and the color changed to murky yellow. After cooling back to room temperature (22 °C) the solvents were evaporated under reduced pressure. The solid yellow-brown residue was dissolved in 15% HCl (10 mL), add chloroform (5 mL) with vigorous stirring, the aqueous layer was separated and extracted with chloroform (3 × 20 mL) and the combined organic layers were dried with brine (20 mL) and further dried over Na_2SO_4, filtered and evaporated under vacuum. Purification by column chromatography (SiO_2, hexanes/EtOAc 6:1) yielded 14 mg of 2- ((3,3,4,4, 5,5-hexafluoro-2-(2-methyl-5-phenylthiophen-3-yl)cyclopent-1-

enyl)methylene)malononitrile (35%) as an orange-red solid. Mp = 102-103 °C (lit. 103-104 °C).[30]

^{1}H NMR (C_6D_6, 600 MHz): δ (ppm) = 1.50 (s, 3H), 5.99 (s, 1H), 7.00 (s, 1H), 7.07 (m, 3H), 7.30 (d, 2H, *J* =7 Hz).[30]

1,2-bis-(3-(5-Chloro-2-methylthienyl))perfluorocyclopentene (**3.5**)

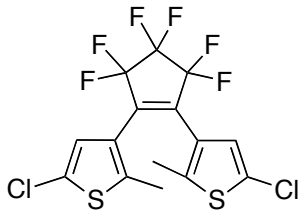

A solution of 3-bromo-5-chloro-2-methylthiophene (3.00 g, 14.2 mmol) in anhydrous THF (100 mL) was cooled in an acetone/dry-ice bath to -78 °C under a nitrogen atmosphere and treated with *n*-BuLi (5.7 mL, 2.5 M in pentane, 28.2 mmol) drop-wise via syringe until TLC provided no evidence of the starting material. The resulting suspension was stirred at this temperature for 15 min upon which octafluorocyclopentene (1.0 mL, 7.1 mmol) was added in one portion using a syringe previously cooled on dry ice. The solution was stirred at -78 °C for 1h. The cooling bath was removed and the reaction was allowed to warm to room temperature (22 °C) at which temperature it was stirred for an additional 30 min. After quenching with saturated aqueous NH_4CI (100 mL), the aqueous layer was separated and extracted with Et_2O (3 ×7 5 mL). The combined organic layers were washed with water, followed by brine, and then dried over Na_2SO_4 and filtered. The solution was evaporated to dryness under vacuum. Purification by column chromatography (SiO_2, hexanes) yielded 3.23 g of 1,2-

bis-(3-(5-chloro-2-methylthienyl))perfluorocyclopentene (52%) as a white solid. Mp = 149-150 °C (lit. 149-150 °C).[30]

^{1}H NMR ($CDCl_3$, 600 MHz): δ (ppm) = 1.88 (s, 6H), 6.88 (s, 2H). [30]

1,2-bis-(2-Methyl-5-formyl-3-thienyl)perfluorocyclopentene (**3.6**)

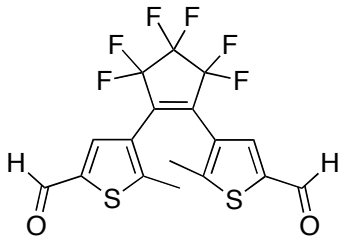

A solution of 1,2-bis-(3-(5-chloro-2-methylthienyl))perfluorocyclopentene (350 mg, 0.80 mmol) in anhydrous THF (50 mL) was cooled in an acetone/dry-ice bath to -78 °C under a nitrogen atmosphere and treated with t-BuLi (1.0 mL, 2.4 M in hexane, 2.2 mmol) drop-wise via syringe until TLC provided no evidence of the starting material. Anhydrous DMF (0.25 mL, 3.2 mmol) was added dropwise by a syringe and the resulting suspension was stirred at -78 °C for 15 min. The cooling bath was removed and the reaction was allowed to warm to room temperature (22° C) and stirred for an additional 1 h. After quenching with saturated aqueous NH_4CI (50 mL) the aqueous layer was separated and extracted with Et_2O (3 × 50 mL). The combined organic layers were washed with water, followed by brine, and then dried over Na_2SO_4 and filtered. The solution was evaporated to dryness under vacuum. Purification by column chromatography (SiO_2, hexanes/EtOAc 4:1) yielded 361 mg of 1,2-bis-(2-methyl-5-formyl-3- thienyl)perfluorocyclopentene (39%) as a light yellow solid. Mp = 182-183 °C (lit. 182-183 °C).[38]

^{1}H NMR ($CDCI_3$, 600 MHz): δ (ppm) = 2.03 (s, 6H), 7.73 (s, 2H), 9.85 (s, 2H).[38]

1,2-bis-(2-Methyl-5-(2,2-dicyanoethenyl)-3-thienyl)perfluorocyclopentene (**3.2o**)

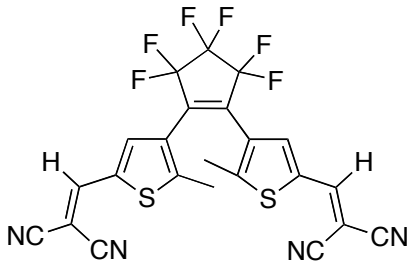

To a 5 mL round bottom flask 1,2-bis-(2-methyl-5-formyl-3-thienyl) perfluorocyclopentene (65 mg, 0.15 mmol) was suspended in absolute ethanol (1.5 mL) with malonodinitrile (20 mg, 0.30 mmol) and a catalytic amount of piperidine (2 drops of a stock solution containing 1 drop of amine in 2 mL absolute ethanol). The reaction was heated to reflux for 3 h afterwhich, the brown solution was cooled to room temperature and the solvent was removed under vacuum. The crude product was triturated with methanol which resulted in the formation of pale yellow crystals of 1,2-bis-(2-methyl-5-(2,2-dicyanoehthenyl)-3-thienyl)perfluorocyclopentene, which were filtered and dried under vacuum (55 mg, 69%). Mp = 205-207 °C (lit. 207-209 °C).[38]

^{1}H NMR ($CDCI_3$, 600 MHz): δ (ppm) = 2.14 (s, 6H), 7.64 (s, 2H), 7.77 (s, 2H).[38]

3.7.4 NMR Binding studies

3.7.4.1 Binding Studies for 1.24o and Karstedt's catalyst

A stock solution (0.36 M) of Karstedt's catalyst was made by diluting Karstedt's catalyst (0.36 mL , 0.1 M in divinyltrimethylsilane) in C_6D_6 (0.64 mL). In a separate NMR tube **1.24o** (10 mg, 0.018 mmol) was diluted in C_6D_6 (0.6 mL), successive equivalents of Karstedt catalyst was added such that each 0.05 mL was equal to 0.1 equivalent, ^{1}H NMR spectra were taken after the addition of the following equivalents 0, 0.2, 0.4, 0.7, 1, 1.5, 2. See appendix for raw data.

3.7.4.2 Binding studies for 2.4 and Karstedt's catalyst

A 0.30 M stock solution of Karstedt's catalyst was made by diluting Karstedt's catalyst (0.30 mL, 0.1 M in divinyltrimethylsilane) in C_6D_6 (0.7 mL). In a separate NMR tube **1** (2mg, 0.010 mmol) was diluted in C_6D_6 (0.6 mL), successive equivalent of Karstedt's catalyst was added such that each 0.1 mL was equal to 0.3 equivalent, ^{1}H NMR spectra were taken after the addition of the following equivalents 0.3, 0.6, 0.9, 1.2, 1.5, 2.1, 3. The appearance of a doublet that is attributed to the bound phenyl protons was followed. See appendix for raw data.

3.7.4.3 Binding studies for 1.25o and Karstedt's catalyst

A 0.30 M stock solution of Karstedt's catalyst was made by diluting Karstedt's catalyst (0.30 mL , 0.1 M in divinyltrimethylsilane) in C_6D_6 (0.7 mL). In a separate NMR tube **1.25o** (4 mg, 0.010 mmol) was diluted in C_6D_6 (0.6 mL), successive equivalent of Karstedt's catalyst was added such that each 0.1 mL was equal to 0.1 equivalent, ^{1}H

NMR were taken after the addition of the the following equivalents 0, 0.15, 0.30, 0.6, 1.2, 1.8, 3. See appendix for raw data.

3.7.4.4 Binding studies for 3.1o and 3.1c with Karstedt's catalyst

To a solution of **3.1o** (3 mg, 0.005 mmol) in 0.45 mL of deuterated solvent (15% NO_2CD_3 in C_6D_6) Karstedt's catalyst in xylenes was added (0.1 mL, 0.01 mmol). A seconde solution of **3.1o** (3 mg, 0.005 mmol) in 0.45 mL of deuterated solvent (15% NO_2CD_3 in C_6D_6) was irradiated with 365 nm light for 15 min (generating **3.1c**). To this solution Karstedt's catalyst in xylenes was added (0.1 mL, 0.01 mmol). ^{1}H NMR spectrums were taken for each solutions.

3.7.4.5 Binding studies for 3.2c and 3.2c

A solution of **3.2o** (5 mg, 0.01 mmol) in C_6D_6 (0.7 mL) was divided into two equal portions. One portion was irradiated with 313 nm light for 10 min. After which, Karstedt's catalyst in siloxane was added (0.1 mL, 0.01 mmol) to each solution. ^{1}H NMR spectrums were taken for each solution.

4 CONCLUSIONS AND FUTURE PERSPECTIVES

Release coatings provide a non-stick backing for everything from stamps to band-aids. They are made of polysiloxanes, which are made by hydrosilylation reactions. Hydrosilylation reactions are catalyzed by platinum catalysts, of which Karstedt's catalyst is the most widely used industrially. One of the most significant challenges in the manufacturing of release coatings is the need for long bath lives of the starting materials. This is achieved by inhibiting the active catalyst, which can then be activated by heating. Heating is a very inefficient way of initiating a reaction. As an alternative, light can be used to initiate reactions. A much more energy efficient method could be achieved by inhibiting the catalyst with a molecule that can be made inactive with light instead of heat.

The dithienyl-based molecular switches are particularly well-suited to the development of photoreactive systems since they have well-behaved photochromic properties and increased thermal stability of both of the isomers compared to other systems such as azobenzenes. Dithienylethene derivatives exhibit significant differences between their ring-open and ring-closed forms. Upon exposure to the appropriate light source the isomerization results in changes to the π-bond arrangement of the molecules.

Electron deficient olefins are known to inhibit Karstedt's catalyst. It was speculated that by modifying a dithienylethene to include an electron deficient double bond so that in one form a double bond is present and in another form it is absent, control over the initiation of Karstedt's catalyst with light may be achieved.

In *Chapter 2*, a series of model inhibitors based on the DCTE architecture were synthesized and tested for inhibition of Karstedt's catalyst. The dicyanoethylene moiety was found to be inefficient at inhibiting the catalyst and only the nitro-substituted inhibitor was found to inhibit this catalyst. Based on these results, DCTE **1.24o** was synthesized but was found not to be an inhibitor of the catalyst, most likely a result of the added steric bulk of the hexafluoro ring. More importantly, a reliable method for determining the inhibition of Karstedt's catalyst was developed and considerations for future experiment are outlined in *Chapter 2*.

In Chapter 3, the interaction between the catalyst and the inhibitor was investigated by ^{1}H NMR spectroscopy. The interaction of several new potential inhibitors as well as the previously studied inhibitors with Karstedt's catalyst were evaluated. However, binding affinities could not be calculated as a result of the complex kinetics of Karstedt's catalyst. The model compound which was shown to inhibit hydrosilylation reactions was observed to have a slow exchange with the catalyst, and molecule **1.24o**, which was not a Karstedt inhibitor, was observed to have a fast exchange with the catalyst. Of the three new molecules that were evaluated all but one was shown to interact with Karstedt's catalyst, however this molecule's PSS was too low for practical use as a photoswitchable Karstedt catalyst inhibitor. Nevertheless, ^{1}H NMR spectroscopy was successful as a screening tool for potential Karstedt catalyst inhibitors as the interaction with the catalyst can be assessed readily and efficiently.

Although no DCTE was found to be suitable as a photoswitchable Karstedt catalyst, this thesis provided the necessary groundwork for future research in this area. Three important conclusions from the work presented are summarized below.

1. The kinetics of hydrosilylation reactions catalyzed by Karstedt's catalyst are complicated and it is not possible to obtain rate constants.

2. Subtle differences in inhibition and reaction rates can not be quantified as a result of (1).

3. ^{1}H NMR spectroscopy is a useful screening tool for potential Karstedt catalyst inhibitors.

In summary, this thesis presented novel approaches to the inhibition of Karstedt's catalyst. Model compounds with varying degrees of electron-deficient double bonds showed the more electron-deficient the double bond, the better the inhibition of Karstedt's catalyst. However, a thienyl based molecular switch did not show any significant differences in inhibition between open and closed-isomers most likely because of steric bulk. Furthermore, the nature of the interaction between catalyst and inhibitor was characterized by ^{1}H NMR spectroscopy, and it was shown that complexes that were longer lived were more likely to inhibit Karstedt's catalyst. Most importantly, the characteristics necessary for a photoswitchable inhibitor are now well defined and the method for determining that inhibition is clearly laid out.

5 APPENDIX

Table 5.1 Spectral data for the binding of Karstedt's catalyst and **1.24.**

Equivalents of catalyst	δ (ppm)	δΔ
0	6.630	0
0.2	6.619	0.011
0.4	6.608	0.022
0.7	6.596	0.034
1	6.586	0.044
2	6.567	0.063

Table 5.2 Spectral data for the binding of Karstedt's catalyst and **2.4**

Equivalents of catalyst	Ratio of bound 2.4:unbound 2.4
0	0
0.3	0.44
0.6	0.78
0.9	1.12
1.2	1.31
1.8	1.46
3	1.52

Table 5.3 Spectral data for the binding of Karstedt's catalyst and **1.25o**

Equivalents of catalyst	Ratio of bound **1.25o**: unbound **1.25o**
0	0
0.15	0.21
0.3	0.50
0.6	0.65
1.2	0.85
1.8	1.04
3	1.45

REFERENCE LIST

1. http://www.dowcorning.com/content/publishedlit/30-1129-01.pdf

2 Stein J., and Eckberg R. P., "Additives and UV Curable Silicone Release Coatings and Controlled Release", *Journal of Industrial Textiles*, 20 , 1990, p. 24-42.

[3] *Concise polymeric materials encyclopedia* (Ed.: Salamone, J.), CRC Press, Florida 1998, p 1459.

[4] *Silicon Based Inorganic Polymers* (Ed.: De Jaeger, R., and Gleria, M.), Nova Science Publishers, 2007, Hauppauge NY, p. 158.

[5] *Inorganic Polymers* (Ed.: Mark, J. E., Allcock, H.R., West, R.), Oxford University Press US, 2005 p. 4.

[6] US Patent 5432006. **1995**. Kessel C.R., and Melancon, K. C., *Solventless silicone release coating*.

[7] *Handbook of Polymer Research: Monomers, Oligomers, Polymers and Composites*, (Ed.: Pethrick, R.A., Ballada, A. Zaikov, G.E.), Nova Publishers, Hauppauge NY, 2007 p. 58.

[8] Lappert, M. and Scott, F., "The reaction pathway from Speier's to Karstedt's hydrosilylation catalyst", *Journal of Organometallic Chemistry,* **1995**, 492, Cll-C13.

[9] Stein, J., "In situ determination of the active catalyst in hydrosilylation reactions", *J. Am. Chem. Soc.,* **1999**, 121, 15, p. 3693-3703.

[10] *Hydrosilylation: A Comprehensive Review on Recent Advances*, Marciniec, B., Springer, Poland, 2009, p. 4.

[11] Lewis, L. N., "Hydrosilylation catalysts derived from cyclodextrin organometallic platinum inclusion compounds and their use in command-cure applications," *J. Inorg. Organomet. Polym.*, **1996,** 6, 2, p. 123-144

[12] *Hydrosilylation: A Comprehensive Review on Recent Advances*, Marciniec, B., Springer, Poland, 2009, p. 4.

[13] US Patent 4774111. **1988**. Lo, P.K., *Heat-curable silicone compositions comprising fumarate cure-control additive and use thereof*.

[14] US Patent 4448815. **1984**. Grenoble, M. E., *Eckberg, R.P. Multi-component solventless silicone release coating system*.

[15] *Concise polymeric materials encyclopedia* (Ed.: Salamone, J.), CRC Press, Florida 1998, p 1460.

[16] Sprengers, J. W., de Greef, M.A., Duin, M., and Elsevier, C.J. "Stable platinum(0) catalysts for catalytic hydrosilylation of styrene and synthesis of [Pt(Ar-bian)(eta(2)-alkene)] complexes," *Eu. J. of Inorg. Chem,* **2003**, 20, p. 3811-3819.

[17] Lewis, L.N., Stein, J., Colborn, R.E., Gao, Y., and Dong, J. "Chemistry of Maleate and fumarate inhibitors," *J. Organomet. Chem*, **1996**, 521, p. 221-227.

[18] Sprengers, J. W., Agerbeek, M.J., and Elsevier, C.J. "Synthesis and crystal structures of zerovalent platinum η2-fumarate bis(norbornene) complexes and their application as hydrosilylation catalyst," *Organometallics*, **2004**, 23, p. 3117-3125

[19] Steffanut, P., Osborn, J.A., DeCian, A., and Fisher, J. "Efficient homogeneous hydrosilylation of olefins by use of complexes of Pt^0 with selected electron-deficient olefins as ligands," *Chem. Eur. J.,* **1998**, p. 2008-2017.

[20] http://www.radtech-europe.com/files_content/oestreichpapermay.pdf

[21] Irie, M., "Photochromism: Memories and Switches," *Chem. Rev*., 5, **2000**.

[22] H. Bouas-Laurent, H. Dürr, "Organic photochromism", *Pure Appl. Chem*. **2001**, *73*, 639-665.

[23] Griffiths, J., "Photochemistry of azobenzene and its derivatives," *Chem. Soc. Rev*. **1972**, 1, 481 - 493.

[24] Feringa, B.L., Wolter, J.,F., and de Lange, B., "Organic materials for reversible optical data storage," *Tetrahedron*, **1993,** 49, p. 8267-8310.

[25] *Photochromism: molecules and systems* (Eds.: H. Dürr, H. Bouas-Laurent), Elsevier, Amsterdam, **2003**, p.1044.

[26] Kaieda, T., "Efficient Photocyclization of Dithienylethene Dimer, Trimer, and Tetramer: Quantum Yield and Reaction Dynamics," *J. Am. Chem. Soc*, 2002, 124, p. 2015-2024.

[27] Tian, H., Yang, S. J., "Recent progresses on diarylethene based photochromic switches," *Chem. Soc. Rev.*, **2004**, 33, 85-97.

[28] Peters, A., Vitols, C., McDonald, R., Branda, N. R., "Novel Photochromic Compounds Based on the 1-Thienyl-2-vinylcyclopentene Backbone," *Org. Lett.,* **2003**, 5, p. 1183-1186.

[29] Wüstenberg, B., Branda, N. R., "A Photoswitchable Donor–π–Acceptor System Based on a Modified Hexatriene Backbone," *Adv. Mater.*, **2005**, 17, p. 2134-2138.

[30] Adams, M. W., **2007**, *Investigating the Refractive Index Change of Donor -pi-Linker-Acceptor Photoresponsive Materials,* [M.Sc. Thesis], Burnaby, Simon Fraser University.

[31] Buisine, O., Berthon-Gelloz, G., Brière, J.F., Stérin, S., Mignani, G., Branlard, P., Tinant, B., Declercq, J.P., and Markó, I.E. "Second generation N-heterocyclic carbene–Pt(0) complexes as efficient catalysts for the hydrosilylation of alkenes," *Chem. Commun.,* **2005**, 3856–3858.

[32] Wang, S., Ren, Z., Cao, W. and Tong, W., "The knoevenagel condensation of aromatic aldehydes with malononitrile or ethyl cyanoacetate in the presence of CTMAB in water", *Syn. Comm.*, **2001**, 31, p. 673-677.

[33] Hosseini-Sarvari, M., "Solvent-free Knoevenagel condensations over TiO2," *Chin. J. Chem*, **2007**, 25, p. 1563-15

[34] K. Hirose, "A practical guide for the determination of binding constants," *J. Inclusion Phenom. Macrocyclic Chem*, **2001**, *39*, p. 193-209.

[35] *Modern physical organic chemistry*, Anslyn, E. V., and Dougherty, D.A., University Science Books, **2006**, p. 218.

[36] Coqueret, X., Wegner, G., "Platinum-catalyzed hydrosilylation of allyl aryl ethers: kinetic investigation at moderately high dilution," *Organometallics,* **1991**, 10, 3139.

[37] Jeremy Finden, Post Doctoral Fellow 2006-2007, Branda Lab. University of Simon Fraser.

[38] Gilat, S. L., Kawai, S. H., Lehn, J.-M.,"Light-triggered electrical and optical switching devices," **1993**, 18, p. 1439-1442.